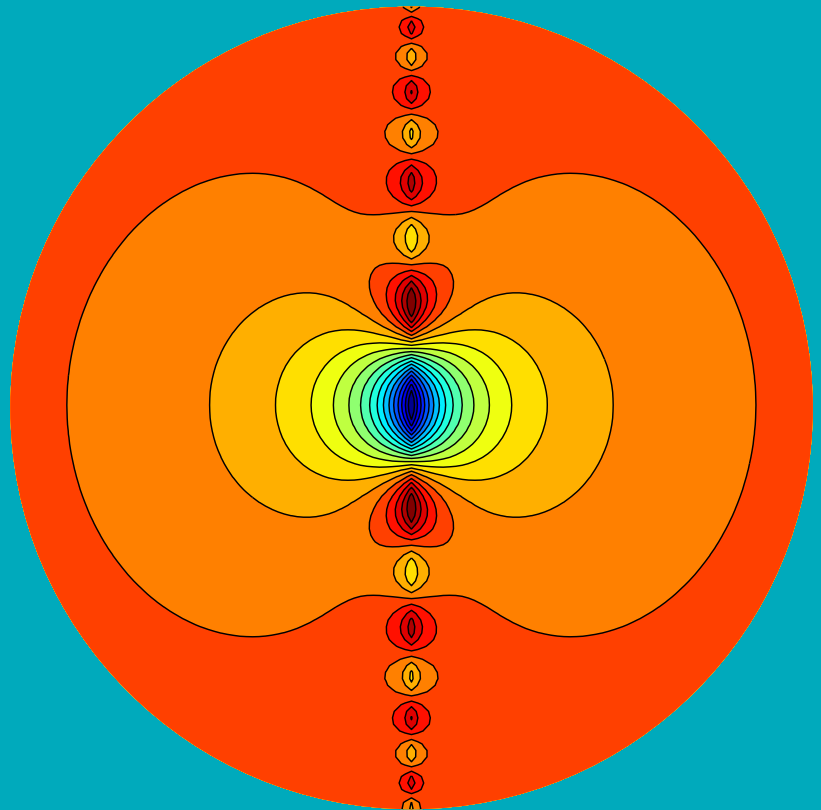


Department of Radio Science and Engineering

Complex electromagnetic responses from simple geometries

Henrik Kettunen



Complex electromagnetic responses from simple geometries

Henrik Kettunen

Doctoral dissertation for the degree of Doctor of Science in Technology to be presented with due permission of the School of Electrical Engineering for public examination and debate in Auditorium S5 at the Aalto University School of Electrical Engineering (Otakaari 5L, Espoo, Finland) on the 15th of December 2011 at 12 noon.

Aalto University
School of Electrical Engineering
Department of Radio Science and Engineering

Supervisor

Professor Ari Sihvola

Instructor

Doctor Henrik Wallén

Preliminary examiners

Professor Christian Brosseau, Université de Bretagne Occidentale, Brest, France

Professor Daniel Sjöberg, Lund University, Sweden

Opponent

Professor Andrea Alù, The University of Texas at Austin, USA

Aalto University publication series

DOCTORAL DISSERTATIONS 106/2011

© Henrik Kettunen

ISBN 978-952-60-4337-1 (pdf)

ISBN 978-952-60-4336-4 (printed)

ISSN-L 1799-4934

ISSN 1799-4942 (pdf)

ISSN 1799-4934 (printed)

Unigrafia Oy

Helsinki 2011

Finland

The dissertation can be read at <http://lib.tkk.fi/Diss/>

Author

Henrik Kettunen

Name of the doctoral dissertation

Complex electromagnetic responses from simple geometries

Publisher School of Electrical Engineering**Unit** Department of Radio Science and Engineering**Series** Aalto University publication series DOCTORAL DISSERTATIONS 106/2011**Field of research** Electromagnetics**Manuscript submitted** 14 June 2011**Manuscript revised** 19 October 2011**Date of the defence** 15 December 2011**Language** English **Monograph** **Article dissertation (summary + original articles)****Abstract**

The electromagnetic properties of a material arise from its intrinsic microstructure, which may often be very complex. However, materials are usually characterized more simply using macroscopic material parameters, electric permittivity and magnetic permeability. This thesis considers the principles of material modeling from the electromagnetics point of view. The analysis is mostly based on electrostatics. The aim of the thesis is to enhance the understanding of the interaction between matter and the electromagnetic fields, and further, the relation between matter and geometry.

The contents of the thesis can be divided into three parts. The first part discusses the concepts of polarization and polarizability and considers the electric responses of particles with different geometries. Polarizabilities of a three-dimensional hemisphere and a two-dimensional half-disk are solved.

The second part studies negative material parameters. The emphasis lies on negative permittivity. Interfaces between permittivities of opposite signs are found supporting surface plasmons, or electrostatic resonances. The occurrence of these resonances is especially studied for a hemisphere and a half-disk. Moreover, it is shown that sharp edges with negative permittivity may support unphysically singular field modes, which in numerical simulations can result in non-convergent solutions. The most efficient way to overcome this problem in computational modeling is to slightly round all sharp corners.

The third part focuses on homogenization of composite media. Effective material parameters modeling the response of a thin dielectric composite slab are retrieved. Computational homogenization techniques and their limitations are studied. The results indicate that for a successful homogenization, the unit cells of the slab must remain very small compared with the wavelength. Also, the boundary layers of the slab show higher effective permittivity than the corresponding bulk medium.

Keywords permittivity, polarizability, negative material parameters, surface plasmon resonances, metamaterials, homogenization, composite media

ISBN (printed) 978-952-60-4336-4**ISBN (pdf)** 978-952-60-4337-1**ISSN-L** 1799-4934**ISSN (printed)** 1799-4934**ISSN (pdf)** 1799-4942**Location of publisher** Espoo**Location of printing** Helsinki**Year** 2011**Pages** 134**The dissertation can be read at** <http://lib.tkk.fi/Diss/>

Tekijä

Henrik Kettunen

Väitöskirjan nimi

Yksinkertaisten geometrioiden synnyttämät monimutkaiset sähkömagneettiset vasteet

Julkaisija Sähkötekniikan korkeakoulu**Yksikkö** Radiotieteen ja -tekniikan laitos**Sarja** Aalto University publication series DOCTORAL DISSERTATIONS 106/2011**Tutkimusala** Sähkömagnetiikka**Käsikirjoituksen pvm** 14.06.2011**Korjatun käsikirjoituksen pvm** 19.10.2011**Väitöspäivä** 15.12.2011**Kieli** Englanti **Monografia** **Yhdistelmäväitöskirja (yhteenvedo-osa + erillisartikkelit)****Tiivistelmä**

Aineen sähkömagneettiset ominaisuudet määräytyvät sen sisäisestä mikrorakenteesta, joka voi usein olla hyvinkin monimutkainen. Tavallisesti materiaaleja kuitenkin mallinnetaan yksinkertaisemmin makroskooppisten materiaaliparametrien, sähköisen permittiivisyyden ja magneettisen permeabilisuuden, avulla. Väitöskirjassa perehdytään materiaalien mallinnukseen sähkömagnetiikan näkökulmasta. Analyysi perustuu pitkälti sähköstatiikan yhtälöihin. Tutkimuksen tavoitteena on lisätä ymmärrystä aineen ja sähkömagneettisten kenttien välisestä vuorovaikutuksesta, ja edelleen aineen ja geometrian välisestä yhteydestä.

Sisällöllisesti väitöskirja voidaan jakaa kolmeen aihealueeseen, joista ensimmäinen perehtyy polarisaation ja polarisoituvuuden käsitteisiin ja käsittelee erimuotoisten kappaleiden sähköisiä vasteita. Erityisesti esitetään ratkaisut kolmiulotteisen puolipallon ja kaksiulotteisen puolipyörän polarisoituvuuksien laskemiseksi.

Toinen osa käsittelee negatiivisia materiaaliparametreja keskittyen lähinnä negatiiviseen permittiivisyyteen. Positiivisen ja negatiivisen permittiivisyyden välisellä rajapinnalla voi esiintyä niin sanottuja pintaplasmonia, eli sähköstaattisia resonansseja. Näiden resonanssien esiintymistä tutkitaan erityisesti puolipallon ja puolipyörän tapauksissa. Lisäksi näytetään, että terävien nurkkien yhteydessä esiintyvät kenttämuodot voivat olla epäfysikaalisen singulaarisia ja estää ratkaisun suppenemisen numeerisissa simulaatioissa. Tehokkain tapa ratkaista ongelma laskennallisen mallinnuksen yhteydessä on hieman pyöristää kaikkia teräviä kulkia.

Kolmas osa perehtyy komposiittimateriaalien mallinnukseen eli homogenisointiin. Työssä pyritään löytämään ohuelle dielektriselle komposiittilevylle sen vastetta mallintavat efektiiviset materiaaliparametrit. Samalla perehdytään laskennallisiin homogenisointimenetelmiin ja näiden rajoituksiin. Onnistuneen homogenisoinnin edellytykseksi havaitaan, että komposiitin yksikkökoppien tulee pysyä erittäin pieninä aallonpituuteen nähden. Lisäksi näytetään, että levyn pintakerrokset antavat korkeamman efektiivisen permittiivisyyden kuin vastaava yhtenäinen materiaali.

Avainsanat permittiivisyys, polarisoituvuus, negatiiviset materiaaliparametrit, pintaplasmoniresonanssit, metamateriaalit, homogenisointi, komposiittimateriaalit

ISBN (painettu) 978-952-60-4336-4**ISBN (pdf)** 978-952-60-4337-1**ISSN-L** 1799-4934**ISSN (painettu)** 1799-4934**ISSN (pdf)** 1799-4942**Julkaisupaikka** Espoo**Painopaikka** Helsinki**Vuosi** 2011**Sivumäärä** 134**Luettavissa verkossa osoitteessa** <http://lib.tkk.fi/Diss/>

Preface

This Thesis was carried out at the Department of Radio Science and Engineering of the Aalto University School of Electrical Engineering.

First of all, I would like to express my gratitude to my supervisor Professor Ari Sihvola, who has given me this opportunity to work and complete my studies and this Thesis in his research group. For me, he has been the source of ideas and motivation. Many thanks also go to my instructor Dr. Henrik Wallén. Considering the practical (scientific, theoretical, computational, technical, bureaucratic, you name it) details of my research, he has been my most important helper and collaborator during these years. I also want to thank my colleague and collaborator Dr. Jiaran Qi.

I want to collectively thank the whole staff of the Department of Radio Science and Engineering, especially the Electromagnetics group, as there are too many people to mention separately. I am thankful of all the help and support I have received in numerous occasions.

Moreover, I wish to thank the pre-examiners, Professor Christian Brosseau and Professor Daniel Sjöberg, for their effort in reviewing this Thesis. Their comments and suggestions are highly appreciated.

My studies have been financially supported by the Graduate School in Electronics, Telecommunications and Automation (GETA). In addition, I have received grants from Tekniikan Edistämmissäätiö and Walter Ahlström Foundation. This support is warmly acknowledged.

Also, I wish to thank my parents for their support during all these years.

Finally, and most importantly, a loving thanks to my wife Leena and our little family, the furry rascals Iiro and Jaska, and the charming lady Suttura.

Espoo, October 19, 2011,

Henrik Kettunen

Contents

Preface	7
Contents	9
List of publications	11
Author's contribution	13
List of abbreviations	15
List of symbols	17
1 Introduction	19
2 Electromagnetics	21
2.1 Time-harmonic fields	22
2.2 Plane waves	22
2.3 Statics and quasi-statics	23
2.4 Complex media	24
3 Of matter and geometry	27
3.1 Polarization of dielectric matter	28
3.2 Polarizability of a dielectric particle	29
3.3 Computation of the polarizability components	31
3.4 Duality relation of 2D geometries	33
4 Negative material parameters	35
4.1 The quest for Negative Index Media	37
4.2 Plasmons and plasmonics	39
4.3 Negative permittivity and electrostatic resonances	40
5 Homogenization of composite media	43

5.1	Classical electrostatic mixing rules	45
5.2	S-parameter retrieval	47
5.3	Field averaging	51
6	Summary of the publications	53
	Bibliography	59
	Errata	67
	Publications	69

List of publications

This Thesis consists of an overview and of the following Publications which are referred to in the text by their Roman numerals.

I H. Kettunen, H. Wallén and A. Sihvola. Polarizability of a dielectric hemisphere. *Journal of Applied Physics*, vol. 102, no. 4, 044105:1–7, August 2007. (incl. Erratum: *J. Appl. Phys.*, vol. 102, no. 11, 119902, 2007.)

II H. Kettunen, H. Wallén and A. Sihvola. Electrostatic resonances of a negative-permittivity hemisphere. *Journal of Applied Physics*, vol. 103, no. 9, 094112:1–8, May 2008.

III H. Kettunen, H. Wallén and A. Sihvola. Electrostatic response of a half-disk. *Journal of Electrostatics*, vol. 67, no. 6, pp. 890–897, November 2009.

IV H. Wallén, H. Kettunen and A. Sihvola. Surface modes of negative-parameter interfaces and the importance of rounding sharp corners. *Metamaterials*, vol. 2, no. 2–3, pp. 113–121, September 2008.

V H. Kettunen, J. Qi, H. Wallén and A. Sihvola. Homogenization of thin dielectric composite slabs: techniques and limitations. *The Applied Computational Electromagnetics Society Journal*, vol. 26, no. 3, pp. 179–187, March 2011.

VI J. Qi, H. Kettunen, H. Wallén and A. Sihvola. Quasi-dynamic homogenization of geometrically simple dielectric composites. *The Applied Computational Electromagnetics Society Journal*, vol. 25, no. 12, pp. 1036–1045, December 2010.

Author's contribution

Publication I: “Polarizability of a dielectric hemisphere”

The research idea for this article was proposed by Prof. Ari Sihvola. The results were derived in collaboration between the Author and Dr. Henrik Wallén. The Author derived most of the presented formulas and computed the presented results. He also prepared the manuscript. Dr. Henrik Wallén and Prof. Ari Sihvola helped improving the paper with their comments.

Publication II: “Electrostatic resonances of a negative-permittivity hemisphere”

This paper extends the analysis of Publication I. The Author computed the results and prepared the manuscript. Dr. Henrik Wallén and Prof. Ari Sihvola helped improving the paper with their comments.

Publication III: “Electrostatic response of a half-disk”

This paper extends the analysis of Publications I and II for a different geometry. The Author computed the results and prepared the manuscript. Dr. Henrik Wallén and Prof. Ari Sihvola helped improving the paper with their comments.

Publication IV: “Surface modes of negative-parameter interfaces and the importance of rounding sharp corners”

This article is a collaboration between the Author, Dr. Henrik Wallén and Prof. Ari Sihvola. It is based on ideas and results related to Publications I and

II. The Author helped deriving the results. Dr. Henrik Wallén prepared the manuscript. The Author also helped improving the paper with his comments.

Publication V: “Homogenization of thin dielectric composite slabs: techniques and limitations”

This paper is based on discussions and collaboration between all listed authors. The Author computed the results and prepared the manuscript. Mr. Jiaran Qi computed reference data using different software for verification of the results and, together with Dr. Henrik Wallén and Prof. Ari Sihvola, helped improving the paper with his comments.

Publication VI: “Quasi-dynamic homogenization of geometrically simple dielectric composites”

This paper is based on discussions and collaboration between all listed authors. Mr. Jiaran Qi computed the results and prepared the manuscript. The Author performed additional simulations using another software for verification of the results and helped improving the paper with his comments.

List of abbreviations

2D	Two-Dimensional
3D	Three-Dimensional
BWM	Backward-Wave Media
DNG	Double-Negative
EMA/EMT	Effective Medium Approximation/Theory
FEM	Finite Element Method
LHM	Left-Handed Media
NIM	Negative Index Media
NRI	Negative Refractive Index
NRW	Nicolson–Ross–Weir
SPP	Surface Plasmon Polariton
SRR	Split-Ring Resonator

List of symbols

B	Magnetic flux density [Vs/m ²]
D	Electric displacement (Electric flux density) [As/m ²]
E	Electric field [V/m]
H	Magnetic field [A/m]
$\overline{\overline{I}}$	Unit dyadic
J	Electric current density [A/m ²]
k	Wave vector [1/m]
k_0	Wave number of vacuum [1/m]
n	Refractive index / Volume number density [1/m ³]
P	Average polarization (Dipole moment density) [As/m ²]
p	Electric dipole moment [Asm]
r	Position vector [m]
t	Time [s]
u	Unit vector
V	Volume [m ³]
v	Volume fraction
z	Normalized impedance / Coordinate in the z-axis [m]
α	Electric polarizability [Asm ² /V]
α_n	Normalized polarizability
$\overline{\overline{\alpha}}$	Polarizability dyadic
ϵ	Electric permittivity [As/Vm]
$\overline{\overline{\epsilon}}$	Permittivity dyadic
ϵ_0	Permittivity of vacuum $\approx 8.8542 \times 10^{-12}$ As/Vm
ϵ_e	Permittivity of environment
ϵ_{eff}	Effective permittivity
ϵ_i	Permittivity of inclusion
ϵ_r	Relative permittivity (Permittivity contrast)
ϵ'_r	Real part of relative permittivity

ϵ_r''	(Negative) imaginary part of relative permittivity
η	Wave impedance [V/A]
λ	Wavelength [m]
μ	Magnetic permeability [Vs/Am]
μ_0	Permeability of vacuum = $4\pi \times 10^{-7}$ Vs/Am
ρ	Electric volume charge density [As/m ³]
σ	Electric conductivity [S/m]
ϕ	Electrostatic potential [V]
χ	Electric susceptibility
ω	Angular frequency [rad/s]

1. Introduction

In introductory electromagnetics, materials are usually modeled with two material parameters, electric permittivity ϵ and magnetic permeability μ . These parameters describe the response of the material in a macroscopic sense. For a homogeneous isotropic material, ϵ and μ are scalar constants. However, if we tune our scale of observation, we find that every seemingly homogeneous material hides an intrinsic heterogeneous structure that gives rise to the characteristics of the material. Sometimes this structure is visually observable, like the grains of sand, sometimes microscopic, like a lattice of molecules or atoms. Obviously, it is quite convenient to embed these complex microscale effects into simple effective macroscopic parameters. In a general case, where the material may show, for instance, anisotropy or non-local effects, two scalar parameters are not enough and extended material models are needed. In order to derive the most suitable effective models with the most accurate parameters, the response of the material's geometric microstructure must be explored. That is, electromagnetic material research, or studying the interaction between matter and electromagnetic fields, eventually comes to studying the relation between matter and geometry. However, like the title of the Thesis implies, the analysis of even the simplest looking geometries may sometimes become rather complicated. In other words, complex geometries are tried to be simplified, but even simple geometries may show complex responses!

The objective of the Thesis is to enhance the fundamental understanding of this matter–geometry relation. We consider responses of single particles and geometries, and finally, we study how a combination of particles could behave as a new effective material.

The Thesis consists of an overview and six peer-reviewed articles. The organization of the Thesis is the following. Chapter 2 gives a brief review of the related electromagnetic theory introducing the most important concepts and the used notation.

The rest of the of the overview can be divided into three parts. First, Chapter 3 considers the fundamental relation between matter and geometry. The Clausius–Mossotti model for dielectric media is discussed and the concept of polarizability [1] as a measure of particle’s electric response is introduced. The related Publications are I and III that by semianalytical methods study the polarizabilities of a hemisphere and a half-disk, respectively.

Chapter 4 then expands the analysis for negative material parameters. The characteristics and possibilities of such ‘negative index media’ are discussed. A brief overview is given on proposed realizations of negative material parameters using novel artificial metamaterials [2–7]. Particles and interfaces with negative permittivity are also found supporting strong resonances called surface plasmons [8]. This phenomenon has recently given rise to an independent field of research called *plasmonics* [9]. The Thesis considers surface plasmons, also referred to as electrostatic resonances [10], from a theoretical point of view. Publications II and III study the plasmonic responses resonances supported by a negative-permittivity hemisphere and a half-disk, respectively. Publication IV gives a general overview of surface modes related to some of the most common canonical geometries and discusses the problems related to computational modeling of negative-permittivity objects.

Chapter 5 considers effective modeling, or homogenization, of composite media [11]. An introduction to classical analytical electrostatic mixing formulas [12] is given. Furthermore, the retrieval of effective permittivity is considered in a dynamic case. Homogenization of dielectric composite slabs is studied in Publications V and VI. Two homogenization methods are discussed, one based on reflection and transmission data, or S-parameters [13, 14], and the other on field averaging.

Finally, Chapter 6 summarizes the main results of the included Publications I–VI.

2. Electromagnetics

The electromagnetic theory builds on four principal laws that are based on empirical observations made in the 19th century and named after Faraday, Ampère and Gauss. These laws were combined and further generalized by James Clerk Maxwell in 1864, which is the reason we nowadays refer to them as the Maxwell equations. A modern way of writing these equations, thanks to vector analysis and Oliver Heaviside, is to present them as partial differential equations as [15]

$$\nabla \times \mathbf{E}(\mathbf{r}, t) = -\frac{\partial \mathbf{B}(\mathbf{r}, t)}{\partial t}, \quad (2.1)$$

$$\nabla \times \mathbf{H}(\mathbf{r}, t) = \mathbf{J}(\mathbf{r}, t) + \frac{\partial \mathbf{D}(\mathbf{r}, t)}{\partial t}, \quad (2.2)$$

$$\nabla \cdot \mathbf{D}(\mathbf{r}, t) = \rho(\mathbf{r}, t), \quad (2.3)$$

$$\nabla \cdot \mathbf{B}(\mathbf{r}, t) = 0, \quad (2.4)$$

where \mathbf{E} is the electric field, \mathbf{B} the magnetic flux density, \mathbf{H} the magnetic field, \mathbf{J} the electric current density, \mathbf{D} the electric flux density, or displacement, and ρ the electric volume charge density. All these quantities are functions of location \mathbf{r} and time t . The equations (2.1)–(2.4) are not perfectly symmetric due to the fact that the magnetic charge and magnetic current remain undiscovered in nature and, therefore, are considered nonexistent. The theory is completed with the constitutive relations, which for homogeneous isotropic media read

$$\mathbf{D} = \epsilon \mathbf{E}, \quad (2.5)$$

$$\mathbf{B} = \mu \mathbf{H}, \quad (2.6)$$

where ϵ is the electric permittivity, μ the magnetic permeability. Moreover, the relation between the current and the electric field is defined by Ohm's law

$$\mathbf{J}_c = \sigma \mathbf{E}, \quad (2.7)$$

where \mathbf{J}_c is the conduction current density and σ the electric conductivity of the medium. In (2.2), term \mathbf{J} includes both the primary source current density and

this conduction current density, which is a secondary field term arisen from a conductive material's response to the electric field. Relations (2.5)-(2.7) describe the interaction between the fields and matter. The permittivity and permeability of a certain material are often expressed as dimensionless parameters ϵ_r and μ_r , relative to the corresponding values of vacuum ϵ_0 and μ_0 , respectively, that is, $\epsilon = \epsilon_r \epsilon_0$ and $\mu = \mu_r \mu_0$.

2.1 Time-harmonic fields

Considering the analysis and actual computation of electromagnetic fields, it is often very convenient to only consider time-harmonic, or monochromatic, fields that oscillate sinusoidally at a certain angular frequency ω . In this case, the fields are treated as complex-valued vectors. In the Thesis, the time convention $e^{j\omega t}$ is used. This enables us to replace all time derivatives by $j\omega$ and further forget the time dependency. The time-harmonic Maxwell equations in a homogeneous isotropic material become

$$\nabla \times \mathbf{E}(\mathbf{r}) = -j\omega\mu\mathbf{H}(\mathbf{r}), \quad (2.8)$$

$$\nabla \times \mathbf{H}(\mathbf{r}) = \mathbf{J}(\mathbf{r}) + j\omega\epsilon\mathbf{E}(\mathbf{r}), \quad (2.9)$$

$$\nabla \cdot \mathbf{D}(\mathbf{r}) = \rho(\mathbf{r}), \quad (2.10)$$

$$\nabla \cdot \mathbf{B}(\mathbf{r}) = 0, \quad (2.11)$$

where the conductivity losses predicted by Ohm's law (2.7) are embedded into the permittivity as

$$\epsilon = \epsilon_0 \left(\epsilon_r' - j \frac{\sigma}{\omega \epsilon_0} \right). \quad (2.12)$$

With the chosen time convention, we write both $\epsilon_r = \epsilon_r' - j\epsilon_r''$ and $\mu_r = \mu_r' - j\mu_r''$ as complex numbers, whose imaginary parts, for passive media, must be zero or negative meaning that the parameters ϵ_r'' and μ_r'' are real and non-negative [16].

2.2 Plane waves

The solutions to (2.8)–(2.11) considered in the Thesis are plane waves whose wavefronts are infinite parallel planes. The waves propagate into a coordinate direction denoted by the wave vector \mathbf{k} that is perpendicular to the constant phase planes. For time-harmonic plane waves, the Maxwell equations simplify

to

$$\mathbf{k} \times \mathbf{E}(\mathbf{r}) = \omega \mathbf{B}(\mathbf{r}), \quad (2.13)$$

$$\mathbf{k} \times \mathbf{H}(\mathbf{r}) = -\omega \mathbf{D}(\mathbf{r}). \quad (2.14)$$

For a plane wave that propagates into the direction of the positive z -axis in a homogeneous and isotropic medium, the wave vector becomes $\mathbf{k} = k \mathbf{u}_z$, where $k = k' - jk''$ is the wave number in the medium and \mathbf{u}_z the z -directed unit vector. The electric field is of the form

$$\mathbf{E}(\mathbf{r}) = \mathbf{E}(z) = \mathbf{E}_0 e^{-jkz}, \quad (2.15)$$

with

$$\mathbf{k} \cdot \mathbf{E}_0 = 0. \quad (2.16)$$

2.3 Statics and quasi-statics

When the frequency ω tends to zero, we are left with static fields and the connection between electricity and magnetism disappears. The physics is then divided into two branches, namely electrostatics and magnetostatics. The electrostatic Maxwell equations are

$$\nabla \times \mathbf{E}(\mathbf{r}) = 0, \quad (2.17)$$

$$\nabla \cdot \mathbf{D}(\mathbf{r}) = \rho(\mathbf{r}), \quad (2.18)$$

whereas the corresponding magnetostatic ones are

$$\nabla \times \mathbf{H}(\mathbf{r}) = \mathbf{J}(\mathbf{r}), \quad (2.19)$$

$$\nabla \cdot \mathbf{B}(\mathbf{r}) = 0. \quad (2.20)$$

As Faraday's law (2.17) in statics states that the electric field is conservative, that is, its curl vanishes, the field can be given as a gradient of a scalar potential function as

$$\mathbf{E}(\mathbf{r}) = -\nabla \phi(\mathbf{r}). \quad (2.21)$$

The analysis reduces to solving the electrostatic potential ϕ which, in source-free space, satisfies the Laplace equation

$$\nabla^2 \phi(\mathbf{r}) = 0. \quad (2.22)$$

The analysis presented in the Thesis is mostly based on electrostatics. However, we consider concepts like negative permittivity, which can only occur with

frequency dispersion. Moreover, we study interaction between the medium and a propagating plane wave. In these cases, the primary assumption is that all considered geometrical details, either the studied separate particles or the intrinsic microscopic heterogeneities of a composite material, are much smaller than the wavelength of the impinging fields. From (2.15), we see that if the electrical size of the studied object with maximum dimension d remains very small and the losses are moderate, that is, $|kd| \ll 2\pi$, the phase of the oscillating field is approximately constant over the whole object, $e^{-jkd} \approx 1$, and the situation is considered locally static. This borderland between statics and dynamics is herein referred to as quasi-statics. The studies reported in the Thesis mostly fall within this area. For instance, Publications II–IV consider objects and geometries with negative permittivity, which is a dynamic phenomenon, with means of electrostatics. That is, by first finding the solution for the potential function from (2.22), polarizabilities of different geometric objects are computed. In addition, Publications V and VI study the homogenization of heterogeneous material. Again, the material interacts with a propagating wave, but since its microscopic details are very small compared with the wavelength, it is modeled effectively homogeneous. An important scope of the Thesis is to find safe and reasonable limits for this homogeneity assumption.

2.4 Complex media

Unfortunately, the constitutive relations written as (2.5) and (2.6) are not applicable in all imaginable cases. For instance, due to the recent boost in the research of artificial metamaterials [2–7], it has become evident that extra attention must be paid to what is really meant by constitutive material parameters. Parameters ϵ and μ are a way to model simple media from the electromagnetic point of view, but if the complexity of the material is increased, two scalar parameters are no longer enough. For instance, in a general bi-anisotropic case, the constitutive relations become [16, 17]

$$\mathbf{D} = \overline{\overline{\epsilon}} \cdot \mathbf{E} + \overline{\overline{\xi}} \cdot \mathbf{H}, \quad (2.23)$$

$$\mathbf{B} = \overline{\overline{\mu}} \cdot \mathbf{H} + \overline{\overline{\zeta}} \cdot \mathbf{E}, \quad (2.24)$$

where the material parameters are given as dyadics [16], or second rank tensors, and the number of individual scalar parameters increases up to 36. The parameters $\overline{\overline{\xi}}$ and $\overline{\overline{\zeta}}$ are introduced to model magnetoelectric coupling, which potentially gives rise to complex material properties such as non-reciprocity

and chirality [17, 18]. Within the scope of the Thesis, the magnetoelectric coupling is not further considered. The materials are also assumed linear and time-invariant.

In Publications V and VI, homogenization of dielectric composite slabs is studied. The purpose is to find an effective macroscopic model for the permittivity to replace the actual intrinsic microstructure of the slab. The applied homogenization model includes the effect of frequency dispersion as

$$\langle \mathbf{D} \rangle = \epsilon_{\text{eff}}(\omega) \langle \mathbf{E} \rangle, \quad (2.25)$$

where $\langle \mathbf{D} \rangle$ and $\langle \mathbf{E} \rangle$ are macroscopic, averaged fields.

However, with increasing frequency, the electrical size of the composite heterogeneities increase and eventually become comparable to the wavelength in the material. In this case, the inhomogeneous microstructure is no longer invisible to the impinging field. This is seen as spatial dispersion, or non-locality, which means that the flux densities \mathbf{D} and \mathbf{B} cannot anymore be defined pointwise from the field values \mathbf{E} and \mathbf{H} , respectively, as in (2.5) and (2.6), but also the behavior of the fields in the vicinity of the point of observation, that is, the spatial derivatives of the fields, must be taken into consideration. For a plane wave, this means that the material properties become dependent on the direction of wave propagation, such as

$$\epsilon = \epsilon(\mathbf{k}). \quad (2.26)$$

For instance, magnetoelectric coupling included in (2.23) and (2.24) is a first-order, and artificial magnetism a second-order effect of weak spatial dispersion [17]. Spatial dispersion strongly limits the applicability of simple homogenization models in case of complex artificial media, especially for the aforementioned metamaterials [19]. Therefore, new characterization methods are constantly under development [20, 21].

3. Of matter and geometry

In our everyday life, we find ourselves surrounded by a great variety of different materials. Many of them exist naturally, such as air, water, stone or wood, but many of them are man-made, like plastic or glass. From the electromagnetics point of view, nature consists of materials that are described by their material parameters, electric permittivity ϵ and magnetic permeability μ . However, compared with the everyday speech, we must be more specific with our definitions. For instance, using terms like wood, rock and metal is not accurate enough, since, for example, copper, silver, and gold have all their own electromagnetic material parameters. Moreover, materials like sand and snow become problematic, as they clearly have an intrinsic heterogeneous structure, that is, they are not homogeneous materials accurately described by two scalar numbers. Instead, they are mixtures of different constituents [12]. Fortunately, in some cases it is possible to model heterogeneous materials using effective material parameters, which is the focus of Chapter 5.

The current chapter, instead, studies the electrostatic response of dielectric matter and further the relation between matter and geometry. However, certain analogies can be drawn between these topics. If we zoom deep enough into the structure of any material, we see that nothing remains homogeneous anymore. Finally, we are facing just elementary particles, like electrons and protons. It becomes evident that the material parameters, ϵ and μ , and furthermore, the whole macroscopic field theory, are only approximative models of the reality of nature.

To understand the idea of modeling dielectric matter with electric permittivity ϵ , we study the concept of polarization. Furthermore, we discuss how the geometry and the permittivity of a macroscopic particle affect its response to an external electric field. This relation is described by a parameter called polarizability.

3.1 Polarization of dielectric matter

By dielectrics, we mean non-magnetic and non-conducting materials with $\mu = \mu_0$ and $\sigma = 0$. Such materials can be portrayed as a collection of positive and negative charge carriers that are bound to the atomic structure and cannot move freely. In the absence of an external electric force, they cancel out each other's effects and the material is observed electrically neutral. When a dielectric material is exposed to an external electric field \mathbf{E} , positive and negative charges experience oppositely directed forces making them form small dipoles with dipole moments \mathbf{p} that are aligned with respect to the external field. We say that the material becomes polarized. In this case, the electric displacement (2.5) can be written as [22]

$$\mathbf{D} = \epsilon \mathbf{E} = \epsilon_0 \mathbf{E} + \mathbf{P}, \quad (3.1)$$

where $\epsilon_0 \mathbf{E}$ corresponds the displacement in vacuum and \mathbf{P} is the average polarization, whose relation to the external field is given by electric susceptibility χ , such as

$$\mathbf{P} = \epsilon_0 \chi \mathbf{E}. \quad (3.2)$$

Thus, it is convenient to embed this effect of polarization into the material parameter permittivity, which becomes of the form

$$\epsilon = \epsilon_0(1 + \chi). \quad (3.3)$$

On the other hand, polarization \mathbf{P} stands for the volume density of the induced dipole moments \mathbf{p} within the material. That is,

$$\mathbf{P} = n \mathbf{p}, \quad (3.4)$$

where n is the number of dipoles per volume unit. The magnitudes and directions of the induced dipoles are proportional to the polarizing electric field. This relation can be written as

$$\mathbf{p} = \alpha \mathbf{E}_{\text{loc}}, \quad (3.5)$$

where the parameter α is called the polarizability and \mathbf{E}_{loc} is the local electric field seen by each individual dipole. In a very dilute material, where the interaction between the dipoles can be neglected, $\mathbf{E}_{\text{loc}} \approx \mathbf{E}$. However, in a more general, denser material, we must take into account that each dipole also feels the effect of its surrounding neighbors. A common, relatively simple model for such field is obtained by considering an empty spherical cavity in the polarized material, where the local field is of the form [22]

$$\mathbf{E}_{\text{loc}} = \mathbf{E} + \frac{1}{3\epsilon_0} \mathbf{P}. \quad (3.6)$$

Finally, following from equations (3.2)–(3.5), for permittivity, we obtain

$$\epsilon = \epsilon_0 + \frac{n\alpha}{1 - \frac{n\alpha}{3\epsilon_0}}, \quad (3.7)$$

which is known as the Clausius–Mossotti, or Lorenz–Lorentz, relation [12]. This equation is a classical example of how the microscopic response of individual dipoles within the material is integrated into one macroscopic parameter, the permittivity ϵ .

3.2 Polarizability of a dielectric particle

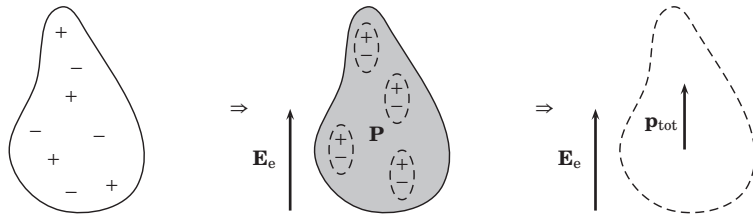


Figure 3.1. When exposed to an external electric field, an electrically neutral dielectric object (left) becomes polarized (middle). In a macroscopic scale, the polarized object can be approximated as an electric dipole (right).

Above, polarization was studied in a microscopic scale as an intrinsic phenomenon characteristic to all dielectric matter. However, in the following, we consider the polarization in a macroscopic sense. We notice that the polarizability α is an important factor in equation (3.7). It is a measure for the response of each individual microscopic dipole that together form the material, whereas permittivity ϵ is a macroscopic measure for the total polarization of the material. Also macroscopic dielectric objects can be polarized by an external electric field, as depicted in Figure 3.1. Let us form a particle by taking a small sample out of our material. The external electric force again induces charges to form microscopic dipole moments within the particle and, due to its finite size, the entire particle can be seen in an averaged sense as one total macroscopic dipole \mathbf{p}_{tot} . We can define the polarizability α also for a finite-size particle as a ratio between the magnitudes of this macroscopic dipole moment and the external polarizing field as

$$\mathbf{p}_{\text{tot}} = \alpha \mathbf{E}_e. \quad (3.8)$$

Considering relation (3.7) in a larger scale, a collection of dielectric particles can be seen as a new material and modeled by an effective permittivity ϵ_{eff} . Analytical formulas for approximating this effective quantity for collections of particles, or mixtures, are known as mixing rules [11, 12]. One could say that the foundations of the theory of mixtures largely lie in the relation (3.7). Moreover, according to this theory, artificial materials with the desired effective permittivities can be designed by tuning the polarizability and the density of the mixture constituents.

The polarizability of a certain particle is largely determined by its geometry [1]. This also means that the macroscopic response of the material is determined by the microscopic geometric details of its internal structure. As Johannes Kepler (1571–1630) has stated: 'Ubi materia, ibi geometria' - 'Where there is matter, there is geometry' [23].

Polarizability α is a convenient measure for the electrostatic response of different particles. However, it must be stressed that we are dealing with a simplified model, as by the definition (3.8), only the dipolar response is taken into account. In reality, the response of the particle may be rather complex, and can only be accurately presented by an infinite sum of higher order multipoles. The higher order terms, however, are significant only in the near vicinity of the particle and rapidly decay as a function of distance. That is, observed from a distance large enough, the polarized particle is seen causing only a dipolar perturbation to the original external field.

Despite the seeming simplicity of definition (3.8), considering dielectric objects with arbitrary ϵ , ellipsoids are the only geometries whose polarizability can be written in a simple analytical closed form [1]. Nevertheless, polarizabilities of various, dielectric or conducting, geometries have been studied using both analytical and numerical methods. In the literature, polarizability studies can be found, for instance, for circular cylinder [24], regular polyhedra [25, 26] and variations of a system of two spheres [27–30]. Also, [31] provides a collection of rather complicated analytical expressions for polarizabilities of various geometries in the limiting case $\epsilon \rightarrow \infty$.

Polarizability has been an important keyword in at least two preceding doctoral theses in the Author's department [32, 33]. The contribution of the Thesis to this field of research are Publications I and III, which study the polarizabilities of a 3D hemisphere and 2D half-disk, respectively. These geometries are special cases of more general configurations simultaneously studied by Pitkonen in [29, 34]. The analysis in [29, 34] is, however, much more mathematical and the obtained exact solutions are given in an integral form. In this compar-

ison, the Author's approach, which follows the idea of [35], is more straightforward yielding approximate results with very reasonable accuracy.

3.3 Computation of the polarizability components

The polarizability is obtained by solving the electrostatic boundary value problem depicted in Figure 3.1, where the object with permittivity ϵ_i is placed into an external uniform electric field \mathbf{E}_e . The constitutive relation (3.1) for the displacement \mathbf{D}_i inside the object is now written as

$$\mathbf{D}_i = \epsilon_r \epsilon_0 \mathbf{E}_i = \epsilon_0 \mathbf{E}_e + \mathbf{P}. \quad (3.9)$$

Herein, we assume that the object is surrounded by vacuum and the dimensionless relative permittivity $\epsilon_r = \epsilon_i/\epsilon_0$ denotes the permittivity contrast between the object and its environment. In a more general case where the object is not surrounded by vacuum but some other homogeneous material, ϵ_0 could simply be replaced with the corresponding permittivity of environment ϵ_e and the relative permittivity defined as the ratio $\epsilon_r = \epsilon_i/\epsilon_e$.

The relation between the polarization \mathbf{P} and the field \mathbf{E}_i inside the object becomes from (3.2) and (3.3)

$$\mathbf{P} = \epsilon_0(\epsilon_r - 1)\mathbf{E}_i. \quad (3.10)$$

As illustrated in Figure 3.1, the average polarization of the particle first arises from the intrinsic microscopic polarization. This relation for an infinite amount of material was simply defined by (3.4). Inside a finite-sized particle, the microscopic dipoles may not, however, be perfectly aligned. In this case, the induced total dipole moment vector \mathbf{p}_{tot} of the particle is obtained by volume integration,

$$\mathbf{p}_{\text{tot}} = \int_V \mathbf{P} dV \quad (3.11)$$

and the polarizability component in the direction of the external field \mathbf{E}_e can be computed from

$$\alpha = \frac{1}{E_e} \int_V \epsilon_0(\epsilon_r - 1)E_i dV. \quad (3.12)$$

Solving the polarizability this way requires that we first have a solution for internal electric field \mathbf{E}_i . In a general case, the analytical solution may not be available. Instead, for numerical computation, this solution is the most straightforward.

Another approach to solve the polarizability is to study the external response of the polarized object. The electrostatic potential ϕ must satisfy the Laplace

equation (2.22), which can be solved by separation of variables in several coordinate systems. The potential outside the object is written as a series expansion and the coefficients of the terms are solved by applying the boundary and interface conditions. The polarizability α can be determined by the dipolar component of the potential. A semianalytical method based on this kind of a series solution for solving the potential for a hemispherical object [35] is improved and applied in Publication I. Publication III then repeats this analysis in two dimensions for a half-disk.

For an arbitrary particle, the polarizability depends on the direction of the external field and to fully determine the polarizability of a 3D object, the polarizability values must be solved in three orthogonal directions. That is, the polarizability can be written as a dyadic $\overline{\overline{\alpha}}$, which collects the information of all three perpendicular polarizability components. For an introduction to dyadics and dyadic operations, see [16]. Also, the equation (3.8) becomes in a more general form

$$\mathbf{p}_{\text{tot}} = \overline{\overline{\alpha}} \cdot \mathbf{E}_e. \quad (3.13)$$

The average polarizability of an object is the average over three perpendicular components, which can also be written by means of the trace [16] of the dyadic $\overline{\overline{\alpha}}$,

$$\alpha_{\text{av}} = \frac{1}{3} \text{tr}(\overline{\overline{\alpha}}) = \frac{1}{3} \overline{\overline{\alpha}} : \overline{\overline{I}}, \quad (3.14)$$

where $\overline{\overline{I}}$ is the unit dyadic.

In 3D, a sphere, which is a special case of an ellipsoid, is the most symmetric of all objects. Due to the spherical symmetry, the polarizability of a sphere reduces to

$$\overline{\overline{\alpha}}_{\text{sph}} = \alpha_{\text{sph}} \overline{\overline{I}}. \quad (3.15)$$

That is, the polarizability of a sphere is determined by one scalar component α_{sph} . Moreover, this component has a closed-form analytical solution. A dielectric sphere with relative permittivity ϵ_r and radius a in a uniform external electric field is a classical example of a 3D electrostatic boundary value problem [15]. The secondary field caused by the sphere is purely dipolar, and the magnitude of the electric field inside the sphere is

$$E_i = \frac{3}{\epsilon_r + 2} E_e. \quad (3.16)$$

As E_i is constant with respect to the spatial coordinates, equation (3.12) gives

$$\alpha_{\text{sph}} = V \epsilon_0 (\epsilon_r - 1) \frac{3}{\epsilon_r + 2}, \quad (3.17)$$

where V is the volume of the sphere. The same solution is easily obtained also by solving the dipole moment of the polarized sphere. This is also the minimum value for average polarizability among all 3D geometries [31, 36].

Moreover, for convenience, instead of the absolute value α , the polarizability is often given as a dimensionless number normalized by the permittivity of the environment and the volume of the object,

$$\alpha_n = \frac{\alpha}{V\epsilon_0}. \quad (3.18)$$

For instance, for the sphere, we usually write

$$\alpha_{\text{sph},n} = 3 \frac{\epsilon_r - 1}{\epsilon_r + 2}. \quad (3.19)$$

Also, the polarizability components of general ellipsoids have analytical expressions [12]. Obtaining simple analytical solutions for general objects, however, seems to be very difficult, if not impossible. Using modern computational methods, it is no problem to compute the polarizability, or related quantities, of any arbitrary object with reasonable accuracy [37]. The emphasis of the Thesis, however, lies on an analytical approach, as we trust that analytical solutions can provide more fundamental understanding on physics and the nature itself.

3.4 Duality relation of 2D geometries

The polarizability of a two-dimensional particle is determined by two perpendicular components α_1 and α_2 . A conjecture has been made that for any 2D geometry, these components are related by [38]

$$\alpha_1(\epsilon_r) = -\alpha_2(\epsilon_r^{-1}). \quad (3.20)$$

The simplest example of a 2D geometry is a disk, a 2D sphere, for which $\alpha_1 = \alpha_2$. The normalized polarizability of the disk reduces to a single component, which is of the form [12]

$$\alpha_{\text{d},n} = 2 \frac{\epsilon_r - 1}{\epsilon_r + 1}. \quad (3.21)$$

We notice that substituting ϵ_r by its inverse ϵ_r^{-1} in (3.21) yields the original polarizability value with a negative sign, which satisfies the conjecture (3.20) in the special case where α_1 and α_2 are equal.

Publication III verifies the relation (3.20) for a half-disk. It is also shown that in the case of a half-disk, all the higher multipole moments are also related by this same duality.

This general duality feature of 2D media [11] was originally reported in works of Keller [39], Dykhne [40], and Mendelson [41], which studied the effective conductivity of two-phase media.

4. Negative material parameters

Let us expand our point of view and consider the possibility of the electromagnetic material parameters to be negative. This may sound like quite an exotic idea, since for a vast majority of all natural materials, $\epsilon \geq \epsilon_0$ and $\mu \geq \mu_0$. However, allowing both $\epsilon, \mu < 0$ gives rise to interesting effects, which originally were theoretically studied by Victor Veselago in the late 1960's [42]. Such 'double-negative' material would support so-called backward waves, whose wave vector \mathbf{k} is antiparallel to the Poynting vector \mathbf{S} , meaning that the phase and the power of the wave are propagating into opposite directions, as depicted in Figure 4.1 [43].

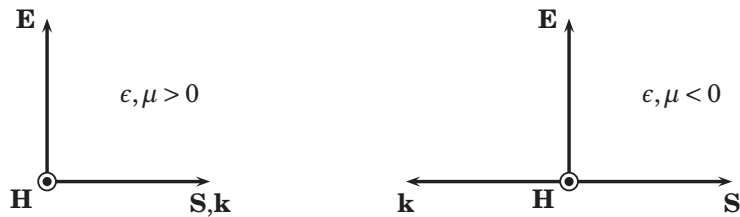


Figure 4.1. Illustration of the wave propagation. An ordinary plane wave in a natural material (left), and a backward wave in a medium where both the permittivity ϵ and the permeability μ are negative (right).

Moreover, the medium would have a negative index of refraction. This is not automatically obvious, since the refractive index is usually written as $n = \sqrt{\epsilon_r \mu_r}$, and it seems that the negative signs of ϵ_r and μ_r should cancel each other. However, the negative branch of the square root must be chosen [42]. Actually, a better way of writing n , especially for numerical evaluation, is

$$n = \sqrt{\epsilon_r} \sqrt{\mu_r}, \quad (4.1)$$

where the square roots are taken separately. In this case, the negative parameters yield (positive) imaginary square roots, which after multiplication give the

wanted minus sign. Instead, the impedance $\eta = \sqrt{\mu/\epsilon}$ remains positive written either way.

Negative permittivity can actually be observed in nature. One example of such a medium is the plasma that occurs in the ionosphere located in the outermost layers of the atmosphere and is ionized by the solar radiation. Moreover, much more tangible examples for an earthly human being are noble metals at optical frequencies [44, 45]. On the contrary, isotropic negative magnetic permeability is not found readily existing anywhere. Therefore, much effort has lately been put in research and development of artificial magnetism. Negative permittivity has also been engineered for lower frequencies by artificial metamaterials [6].

Within the scope of the Thesis, we mainly focus on the negative permittivity. This kind of 'single-negative' medium also offers a stage for fascinating physics. It is found that the interface between permittivities with opposite signs is capable of supporting resonances of sub-wavelength scale. These resonant modes are usually referred to as plasmons. In optics, such an interface exists between a metal and a dielectric, offering new intriguing possibilities for scientists to manipulate light [46]. Also, small particles with negative ϵ may show strong resonant responses [44, 47]. Small metallic nanoparticles, for instance, can have resonances at visible wavelengths and appear in different bright colours. This plasmonic effect has actually been exploited, without the slightest idea of plasmons or modern nanotechnology, already centuries ago when stained glass was made by mixing, for instance, gold and silver particles in the glass. The most famous example of such handcraft is the Lycurgus cup from the 4th century A.D., nowadays held in the British Museum [48].

If the size of the particle is much smaller than the wavelength, the fields in the vicinity of the particle can be considered locally (quasi-)static, even though we would study optical frequencies, which are required for negative ϵ with natural materials. That is, plasmonic resonances are also found by electrostatic analysis as a solution to the Laplace equation (2.22) and, therefore, we also often call them electrostatic resonances [10]. The Thesis studies how the geometry of the particle determines the permittivity value, or values, which yield resonant responses. In a lossless case, where ϵ is purely real and negative, the response may become singular. Even the canonical geometries studied in Publications II and III show quite complex behavior when negative ϵ allowed. This is an essential theme within the Thesis, to which its title also refers.

4.1 The quest for Negative Index Media

It was not until 30 years after Veselago's paper [42] that the negative material parameters really became topical. The famous publication that resurrected Veselago's idea of negative refraction was Pendry's article on the perfect lens [49], which would overcome the diffraction limit of conventional lenses. Figure 4.2 presents the wave refraction as a ray diagram in a slab with refractive index $n = -1$. As the wave refracts negatively, a focus is formed inside the slab and another one on the other side of the slab. That is, the radiation from the source is converged into one point and a perfect image is obtained. Pendry further explained that the focusing is achieved by the evanescent components of the wave, which by negative n are amplified in magnitude.

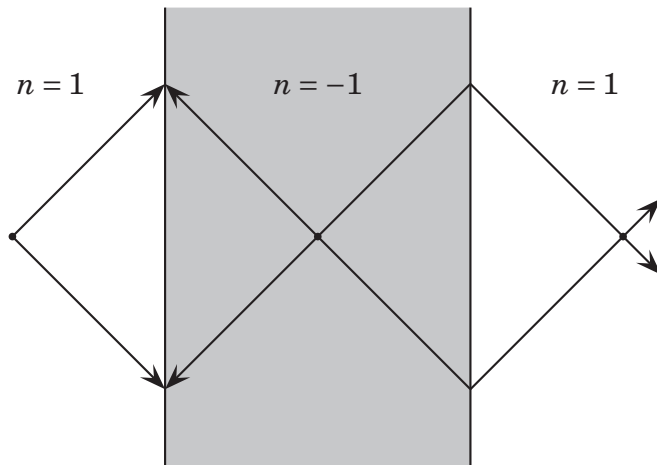


Figure 4.2. Negative refraction makes a perfect lens. The arrows show the direction of the phase propagation

What really started the boom was that the missing medium with negative ϵ and μ was finally available, at least in theory [50]. One could artificially construct a material that would mimic the behavior of such naturally nonexistent medium, at least for a plane wave excitation and for one polarization. Negative permittivity would be achieved by wire media, that is, a lattice of thin metal wires, which can be tuned to imitate the behavior of plasma at microwave frequencies [43], and negative permeability by strong magnetic resonance of small inclusions, which would behave as artificial molecules. The most famous suggestion for this kind of a magnetic particle was the so-called split-ring resonator (SRR) [51]. A little later, the first example was built and experimentally tested [52]. The era of metamaterials had begun.

Since then, numerous research groups have put a lot of effort in the analysis and realization of simultaneously negative material parameters. The desired materials with $\epsilon, \mu < 0$ have also been given many names, such as negative index media (NIM), negative refractive index (NRI) media [2], double-negative (DNG) media [3], backward-wave media (BWM) and, in honor of their discoverer, Veselago media [43]. Also, the name left-handed media (LHM) is often used [5,6]. This sounds natural, since for a backward wave, the $(\mathbf{E}, \mathbf{H}, \mathbf{k})$ triplet becomes left-handed, see e.g. Figure 4.1. However, this term may be confusing [53], since the handedness of the material is usually related to chirality, that is, material's capability to rotate the polarization of a propagating wave, which is an effect of magnetoelectric coupling, discussed in Chapter 2, and not of negative material parameters.

Even though not based on negative material parameters, one cannot leave the famous idea of electromagnetic cloaking [54,55] without mentioning, as it even more increased the interest towards metamaterials. The material model for the cloak was obtained by transformation optics, and soon, the first approximate realization of a metamaterial cloak was introduced [56]. However, already a little earlier, reducing scattering by negative permittivity/permeability metamaterials had been considered [57]. This approach has later been referred to as plasmonic cloaking [58].

In addition to the original wire media and split-ring resonator -based realizations, alternative configurations have been suggested. Metamaterials based on transmission-line techniques are considered widely in the literature [2,4] and a recent doctoral dissertation from the Author's department has contributed to this field of research [59]. Furthermore, by the means of nanotechnology, very small structures aiming at optics can be developed. One of the most famous realizations has been the so-called fishnet structure [60–62].

However, the progress of metamaterials has not been as smooth as one could have hoped. Future will show if the highly intriguing possibilities of metamaterials will ever be realized as functional applications. There are opinions for and against. Among the most severe criticism, even the original conclusions of Veselago have been questioned [63]. In any case, there are still fundamental issues to overcome. For instance, as negative ϵ and μ are based on resonance and strong dispersion, the desired parameter values can be achieved only in a very narrow frequency band [64–66]. Also, especially in the case of the perfect lens, material losses would significantly decrease the focusing effect [67–69].

Furthermore, as metamaterials are supposed to behave as real homogeneous materials, the size of artificial inclusions forming the material must be very

small compared with the wavelength. This requirement is not that easily achieved, especially when the structure is supposed to be resonant [70]. This topic is more thoroughly discussed in Chapter 5, where material homogenization is considered.

4.2 Plasmons and plasmonics

In the following, we focus on non-magnetic media and consider only negative permittivity. As mentioned above, the interfaces between media with opposite signs of ϵ are capable of supporting surface resonances also known as plasmons. These surface plasmon resonances were predicted in 1957 by Ritchie [71] when he studied anomalous energy losses of fast electrons passing through metal films. At optical frequencies, metals can be modeled as a free-electron gas, or plasma, from which the term 'plasmon' clearly derives. A little later, Stern and Ferrell pointed out that on an interface between permittivities of opposite values, the Laplace equation could have an oscillating solution without external excitation [72].

These resonances, or surface plasmons, are oscillations of electron density on a metal-dielectric interface, which are experienced as strong localized enhancements of electric field. Surface plasmons can be excited by light and electromagnetic waves can be coupled to such surfaces. The surface waves that are due to the interaction of the photons of the incident light and the plasmons of the surface are called surface plasmon polaritons (SPP) [8]. The wavelength of these waves is much smaller than the free-space wavelength at the same frequency. Therefore, SPPs offer new possibilities for light confinement and manipulation. In the 21st century, the research of plasmons has actually created a new discipline in physics called plasmonics [9, 46], which has also had a close connection to metamaterials research. Surface plasmon resonances are present, for instance, in the suggested near-field superlens that is not based on negative refraction but only negative ϵ [49]. The performance of the lens is based on the enhancement of the evanescent near-field components by surface plasmon resonances.

Moreover, surface plasmons and plasmonics open a wide range of possible applications. For instance, surface plasmons help improving the resolution and sensitivity in many sensor applications [73]. By the possibility of confining light into sub-wavelength scale, plasmonics may one day lead to a revolution in circuit technology, as the data transfer capacity of optics could be merged

with the small nanoscale size of chip-based integrated circuits [74]. Plasmonics could have many applications also in nano-optics [47] and in biology and medicine, again, for instance, in sensor applications [75]. Plasmonics may one day even be used for cancer treatment, where tumors could be destroyed by heating them using plasmonic nanoparticles injected in blood [76, 77]. Furthermore, plasmonics may even help us save energy, by enhancing the efficiency of LED lighting [78] and photovoltaic cells used in harvesting solar energy [79].

4.3 Negative permittivity and electrostatic resonances

Within the Thesis, we study the resonant response of negative-permittivity particles and geometries. In other words, we consider surface plasmons from a rather theoretical point of view. There is nothing anomalous about plasmonic resonances, since they are valid solutions of the Maxwell equations, and thereby obey the laws of physics [10, 80, 81]. However, they can exist without external excitation. The present analysis is based on electrostatics, that is, we make the locally quasi-static assumption of the particle size being very small compared with the wavelength of the external field. In this case, plasmonic resonances appear as special solutions of the Laplace equation (2.22) and we refer to them as electrostatic resonances. In statics, the solutions do not resonate as a function of time, but as a function of space.

Publications II and III study a negative-permittivity hemisphere and a half-disk, respectively. In the literature, earlier studies of the plasmonic response of a hemisphere can also be found [35]. Publication IV gives an overview of surface modes related to some of the most common canonical geometries.

The simplest example is, again, the sphere. From the polarizability equation (3.17), we notice that with relative permittivity $\epsilon_r = -2$, the response of the sphere becomes singular. This singularity is often referred to as Fröhlich resonance [44]. A deviation from spherical geometry makes this resonance shift from -2 . As shown in Publication IV, ellipsoids, for instance, support three separate resonances whose relation to permittivity is defined by the axis ratio.

This singularity condition for the sphere is also known as 'Mossotti catastrophe' [12]. In the light of the aforementioned fantastic possibilities and application ideas of the plasmonics, this phenomenon seems anything but catastrophic. However, from the viewpoint of computational modeling, we need to be careful, as in some cases, mathematics and physics do not meet, as the solutions can be non-unique and singular. The most problematic case is probably a sharp

corner, or a wedge, which supports resonant edge modes [82]. Instead of a single resonant permittivity value, a continuous spectrum of singularities appears on a certain permittivity range whose breadth depends on the opening angle of the wedge [11, 82, 83]. Moreover, the edge modes of a sharp wedge are unphysically singular since the energy of the electric field becomes infinite [84]. This is a problem when modeling negative-permittivity, or negative-permeability, objects with sharp edges and corners, as numerical methods may not converge in these cases [85].

A numerical integral equation technique was recently introduced for dealing with elliptic problems including non-smooth boundaries with sharp corners [86]. Recent studies [87, 88] suggest that, based on this method, unambiguous and convergent solutions can be obtained also for corners with negative permittivity. However, this method allows an emergence of a complex solution from purely real constituents. This is interpreted to mean that a sharp corner with real but negative permittivity would actually act as an energy absorber [11, 88], which is not consistent with the assumption of the passivity of the material.

The effect of sharp edges is clearly visible in cases of the hemisphere in Publication II and the half-disk in Publication III. A notable thing is that adding moderate material losses does not solve the problem. Instead, rounding the sharp edges is a possible way to remove the unphysical singularities [84]. This important point is also verified by simulations in Publication IV.

5. Homogenization of composite media

Let us finally focus on characterization and effective modeling of heterogeneous composite media [11, 89], in other words, homogenization. If the inhomogeneities of the material are small enough with respect to the wavelengths of the exciting fields, the complex intrinsic microstructure can be forgotten and it is enough to only consider the effective response of the material in a macroscopic scale, as illustrated in Figure 5.1. However, in order to retrieve a reasonable effective model for the studied medium, we need to know the details of its microscopic structure as they eventually give rise to the actual observed material properties, as discussed in Chapter 2. This topic has yielded a preceding doctoral dissertation in the Author's department, as well [90].

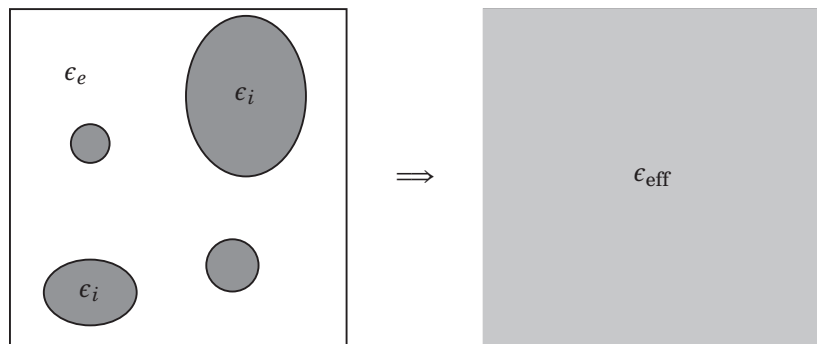


Figure 5.1. The complex microstructure of heterogeneous mixture is replaced by an effectively homogeneous model.

Homogenization theories are needed for the analysis of heterogeneous media, but on the other hand, they can also serve as design tools for novel artificial materials that would even have electromagnetic properties not readily occurring in nature [43]. As stated before, if the scale of observation is small enough, every material starts to look heterogeneous. In natural materials, the intrinsic structure may often be very random, such as in snow, rocks, or biological tissue [12]. In the Thesis, the focus is, instead, on ordered artificial structures that consist

of a periodic lattice of 'building blocks' called unit cells. This is the case with many suggested metamaterials [50]. In practice, these materials are usually designed to work in microwave or even optical frequencies, which sets certain size limitations for their artificial molecules. Homogenization approaches are, however, sometimes used quite freely without paying too much attention on the two fundamental limitations that are the maximum size and the minimum number of unit cells to make the man-made structure really behave as a homogeneous material instead of just a special electromagnetic device performing a certain function.

In a dynamic case, the presented analytical approaches to homogenization have not been very simple [21, 91, 92]. Therefore, the effective parameters are more often retrieved by measurements or simulations. In simulations, the material interaction with a free-space plane-wave, or the dispersion of a single unit cell, can be studied. In real-life measurements, a sample of the studied material is usually placed into a waveguide [93, 94] or a coaxial line [95].

Because the principle in the Thesis is to keep to geometries as simple as possible, we study these fundamental limits of homogenization using a simple cubic lattice of dielectric spheres. That is, our unit cell is a cube with a concentric sphere inside (see e.g. Publication V). Figure 5.2 depicts the particular example considered in the Thesis, which is a lossless dielectric composite slab, whose dimensions are infinite in the transverse plane. In the longitudinal direction, instead, the slab includes only a few layers of unit cells. The presented homogenization studies are based on simulations. The following methods for the retrieval of effective permittivity are considered. The first one is so called Nicolson–Ross–Weir technique [13, 14] that is based on scattering parameters, or S-parameters [96]. The other method is based on averaging of electromagnetic fields. Also, permittivity extraction is studied by computing the dispersion diagram for a single unit cell by eigenfrequency analysis.

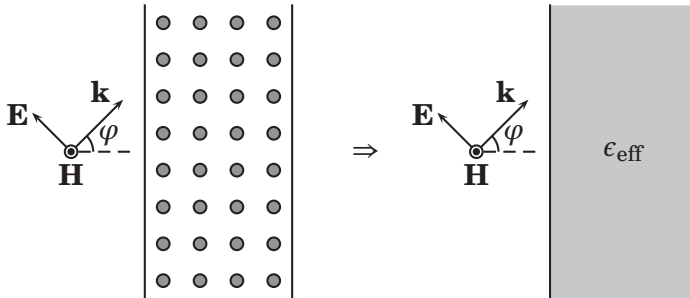


Figure 5.2. A plane wave is incident to a composite slab that is modeled effectively homogeneous.

Both Publications V and VI study the frequency dispersion of the effective permittivity retrieved with different computational methods. Publication V also studies how the thickness, that is, the number of layers in slab, affects the retrieval result. In the static limit, a comparison with classical mixing formulas is made.

5.1 Classical electrostatic mixing rules

Let us consider a non-magnetic dielectric mixture made of inclusions with permittivity ϵ_i embedded into background material with ϵ_e . Permittivities are given as dimensionless numbers relative to ϵ_0 . The inclusions occupy a volume fraction v of the total volume. In a static case, the effective permittivity ϵ_{eff} of the mixture can be approximated by various analytical formulas also known as mixing rules, which are functions of these aforementioned parameters [11, 12].

One of the most famous, and perhaps the simplest one, is the Maxwell Garnett mixing rule [97]

$$\epsilon_{\text{eff}} = \epsilon_e + \frac{3v\epsilon_e(\epsilon_i - \epsilon_e)}{\epsilon_i + 2\epsilon_e - v(\epsilon_i - \epsilon_e)}. \quad (5.1)$$

The Maxwell Garnett formula is obtained by substituting the polarizability of the sphere (3.17) into the Clausius–Mossotti relation (3.7). The principal assumption is that the inclusions are spheres that are polarized and seen as dipoles. The dipolar interaction between the spheres is modeled by the averaged local field (3.6). Therefore, the applicability of the Maxwell Garnett rule is limited to mixtures of separated spheres with a small volume fraction.

Another way to derive the Maxwell Garnett formula is to solve the internal field of a polarized sphere (3.16) and consider the effective permittivity as a ratio of the volume averages of electric displacement \mathbf{D} and the electric field \mathbf{E} in one unit cell [12].

A more accurate mixing formula for a cubic lattice of spheres was derived even before Maxwell Garnett by Lord Rayleigh [98]:

$$\epsilon_{\text{eff}} = \epsilon_e + \frac{3v\epsilon_e}{\frac{\epsilon_i + 2\epsilon_e}{\epsilon_i - \epsilon_e} - v - 1.305 \frac{\epsilon_i - \epsilon_e}{\epsilon_i + 4\epsilon_e/3} v^{10/3}}. \quad (5.2)$$

The Rayleigh formula takes also the quadrupole interaction between of spheres into account and can, therefore, be applied for larger volume fractions than the Maxwell Garnett rule. The most accurate solution for the cubic lattice can be obtained by the method presented McPhedran and McKenzie [99]. The method, being an extension to the Lord Rayleigh formula, is based on a series expansion, where the multipole interactions between the spheres can be taken into account

up to an arbitrarily high order. Also, an explicit formula is derived that includes yet two orders higher multipole interactions than Lord Rayleigh's formula. We refer to this formula as the McPhedran–McKenzie mixing rule. However, the use of all these formulas is strictly limited below the volume fraction $v = \pi/6 \approx 52\%$, where the spheres are already touching each other.

Another famous mixing formula is the one of Bruggeman [100], often referred to as effective medium theory or approximation (EMT/EMA) [11, 101]:

$$(1 - v) \frac{\epsilon_e - \epsilon_{\text{eff}}}{\epsilon_e + 2\epsilon_{\text{eff}}} + v \frac{\epsilon_i - \epsilon_{\text{eff}}}{\epsilon_i + 2\epsilon_{\text{eff}}} = 0. \quad (5.3)$$

Written explicitly for ϵ_{eff} , the (symmetric) Bruggeman formula yields a quadratic equation. The Bruggeman formula works best for random mixtures, where the inclusions are allowed to overlap and form clusters. Therefore, it is not very suitable for the composites considered within the Thesis.

Furthermore, a unified mixing formula can be written as [12]

$$\frac{\epsilon_{\text{eff}} - \epsilon_e}{\epsilon_{\text{eff}} + 2\epsilon_e + \gamma(\epsilon_{\text{eff}} - \epsilon_e)} = v \frac{\epsilon_i - \epsilon_e}{\epsilon_i + 2\epsilon_e + \gamma(\epsilon_{\text{eff}} - \epsilon_e)}, \quad (5.4)$$

which for parameter value $\gamma = 0$, gives the Maxwell Garnett rule (5.1) and with $\gamma = 2$, the Bruggeman formula (5.3). For $\gamma = 3$, (5.4) yields the so-called Coherent potential formula. Instead, parameter value $\gamma = 1$ does not result in any well-known mixing rule.

Mixing rules can also be given for a 2D square lattice of circular inclusions. The 2D version of the unified formula reads [12]

$$\frac{\epsilon_{\text{eff}} - \epsilon_e}{\epsilon_{\text{eff}} + \epsilon_e + \gamma(\epsilon_{\text{eff}} - \epsilon_e)} = v \frac{\epsilon_i - \epsilon_e}{\epsilon_i + \epsilon_e + \gamma(\epsilon_{\text{eff}} - \epsilon_e)}, \quad (5.5)$$

where the parameter values $\gamma = 0, 1$ and 2 correspond to Maxwell Garnett, Bruggeman and the Coherent potential, respectively. Lord Rayleigh also provides a formula for 2D lattice [98], and the most accurate solution is again derived by McPhedran and McKenzie [102].

Figure 5.3 presents the behavior of the aforementioned 3D mixing formulas for inclusion permittivity $\epsilon_i = 20$ and background permittivity $\epsilon_e = 1$ as a function volume fraction v . With small v all formulas give the same result. With this permittivity contrast, Bruggeman starts to deviate from the others already at $v \approx 0.1$, whereas the other three seem to give quite consistent results up to $v \approx 0.3$. However, these three formulas are not supposed to work after $v = \pi/6$, and the formulas of Lord Rayleigh and McPhedran–McKenzie even result in singularities with too large v . Therefore, their curves are plotted only for limited values of v .

These considered mixing rules are only applicable in a static case. However, in practice, effective medium models are also needed in dynamic cases. For in-

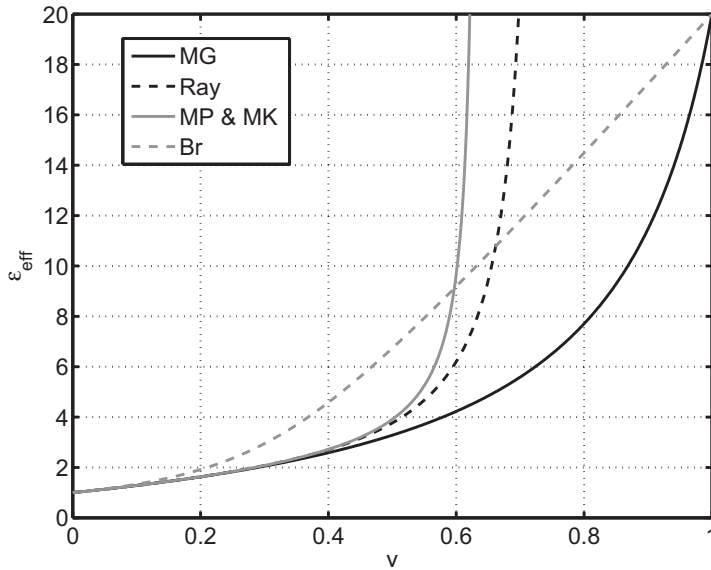


Figure 5.3. Comparison between different mixing rules as a function of volume fraction v with $\epsilon_i = 20$ and $\epsilon_e = 1$: (MG) Maxwell Garnett, (Ray) Lord Rayleigh, (MP & MK) McPhedran & McKenzie and (Br) Bruggeman.

stance, Publication VI computationally studies the dynamic applicability range for the Lord Rayleigh mixing formula when the composite is excited with a plane wave with increasing frequency. Mixing rules including dynamic correction terms would be a fruitful subject for future research. Some extensions for the Maxwell Garnett formula can already be found in the literature [103].

The Author's research group has also studied the performance of classical mixing formulas with plasmonic, negative-permittivity inclusions in an article not included in the Thesis [104].

5.2 S-parameter retrieval

A widely applied method for material parameter retrieval is the so-called S-parameter retrieval technique. It was first introduced in 1970's by Nicolson and Ross [13] and Weir [14], and the method is often referred to as the Nicolson–Ross–Weir (NRW) technique. The technique is suitable for simulations and actual measurements, as it is a non-destructive method based on reflection and transmission data from a material sample. From the obtained two complex scattering parameters [96], S_{11} and S_{21} , it is possible to extract two complex

parameters, that is, permittivity ϵ and permeability μ (see the illustration in Figure 5.4). Originally, the method was developed for determination of parameters for homogeneous materials, but especially in recent years, with some modifications, it has been used for extracting the effective parameters of metamaterials as well [105, 106].

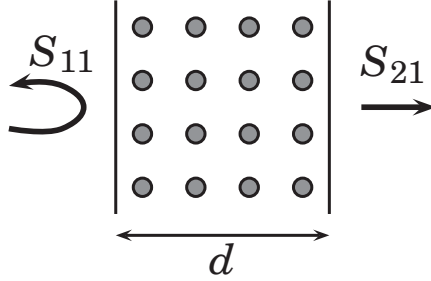


Figure 5.4. S-parameter retrieval method is based on simulated or measured reflection and transmission data, namely the parameters S_{11} and S_{21} , from the material sample.

Unfortunately there are certain issues that complicate the use of the method. Firstly, the material parameter retrieval from S-parameters is ambiguous [14, 106], and usually, some a priori knowledge about the material is needed to resolve the correct branch of the solution. Secondly, for low-loss materials, the retrieval is ill-behaved when the electrical thickness of the material sample becomes an integer multiple of one half-wavelength of the exciting field [95], and thirdly, especially for metamaterials, the retrieved parameter values may sometimes become unphysical [19, 107] showing anomalous dispersion and violating the principles of passivity and causality, that is, the Kramers–Kronig relations [15]. These issues are discussed in more detail in the following.

In the Thesis, we have mostly followed the formulation presented in [106], except for our different time dependency notation $e^{j\omega t}$. It is assumed that the studied composite slab with thickness d , shown in Figure 5.2, can be modeled effectively homogeneous using parameters ϵ and μ . If the slab, surrounded by free space, is excited with a normally incident ($\varphi = 0$) plane-wave, the analyti-

cally derived S-parameters become

$$S_{11} = \frac{\frac{z-1}{z+1}(1 - e^{-j2nk_0d})}{1 - \left(\frac{z-1}{z+1}\right)^2 e^{-j2nk_0d}}, \quad (5.6)$$

$$S_{21} = \frac{\left(1 - \left(\frac{z-1}{z+1}\right)^2\right) e^{-jnk_0d}}{1 - \left(\frac{z-1}{z+1}\right)^2 e^{-j2nk_0d}}, \quad (5.7)$$

where z is the dimensionless impedance normalized to free-space, n is the refractive index and k_0 the free-space wave number. That is, the primary parameters obtained by this retrieval method are z and n . The impedance can be solved from

$$z = \pm \sqrt{\frac{(1 + S_{11})^2 - S_{21}^2}{(1 - S_{11})^2 - S_{21}^2}}, \quad (5.8)$$

where the condition $\Re\{z\} \geq 0$ must be satisfied. The exponential phase factor including the refractive index n can be written as

$$x = e^{-jnk_0d} = \frac{S_{21}}{1 - S_{11} \frac{z-1}{z+1}}. \quad (5.9)$$

When we solve this equation for n , we directly see the first issue that complicates the retrieval. The solution for the real part of the refractive index becomes ambiguous, that is,

$$n = \frac{1}{k_0d} (j \ln x + 2\pi m), \quad (5.10)$$

where m is an integer number denoting the branch of the complex logarithm function. Finally, the relative (effective) material parameters are obtained by

$$\epsilon_r = \frac{n}{z} \quad (5.11)$$

and

$$\mu_r = nz. \quad (5.12)$$

The ambiguity problem was already discussed by Weir [14], where he suggested that the correct branch was determined by measuring the group delay of the signal through the material sample. A more recent, mathematical solution for finding the correct branch was derived by Chen et al. [106]. Also, an algorithm based on the Kramers–Kronig relations is proposed in [108]. The branch selection problem is especially acute in metamaterial characterization when both ϵ and μ are unknown and highly dispersive. Instead, in the case of a dielectric composite, as in the Thesis, the correct branch can be chosen by the condition $\mu_r = nz \approx 1$.

Another issue, more relevant to the Thesis, are the half-wavelength thickness resonances, to which we refer as Fabry–Pérot resonances in Publications V and VI. The problem occurs especially with low-loss materials, where at slab

thickness $\lambda/2$, the reflection coefficient S_{11} can be very close to zero, and the magnitude of the transmission $|S_{21}|$ close to unity. In this case, the retrieval of the impedance z from (5.8) fails. The ill-defined z further ruins the retrieval for both ϵ and μ making them resonant. These resonances should appear exactly at an integer multiple of $\lambda/2$, but for composite media, we have noticed that the effect is more broadband. Instead, the refractive index $n = \sqrt{\epsilon_r \mu_r}$ is unaffected by these resonances, as verified by a mathematical sensitivity analysis in [94].

An iterative method for overcoming the thickness resonance problem was introduced in [95]. Also, in [109], it was noticed that for dielectric media, with $\mu_r = 1$, the ill-behaved impedance z was not needed for solving the permittivity. In other words, physically reasonable ϵ_r can be obtained from the refractive index as

$$\epsilon_r = n^2. \quad (5.13)$$

In Publication VI, we refer to (5.13) as a compensation method.

The third issue related to the material parameters obtained by NRW-technique could be named as an antiresonance problem [110]. Often for metamaterials, or composites with resonant inclusions, one of the retrieved material parameters has a reasonable Lorentz-like curve, but for the other parameter, the curve is inverted. In this case, the dispersion of the real part does not satisfy the laws of causality. Also, the imaginary part of the corresponding parameter has a wrong sign referring to an active material, which means that the retrieved parameters are clearly unphysical. A similar behavior is also observed for lossless composites at Fabry–Pérot resonances in Publications V and VI. However, NRW-technique is widely applied for metamaterial characterization and a lot of results have been published that do not satisfy the requirements of physical material parameters [107].

Nevertheless, despite the retrieval method, the actual problem seems to be in the applied homogenization model. If the unit cells do not remain small enough with respect to the wavelength, these inhomogeneities of the material microstructure eventually give rise to spatial dispersion, that is, non-local effects that cannot be correctly captured using a local material model with only two complex parameters, ϵ and μ , that we can resolve using the conventional NRW method. It is claimed that the parameters retrieved using NRW technique do not represent the actual characteristic (effective) material parameters, but something else [19, 107]. For instance, in [21], term ‘equivalent material parameters’ is used.

5.3 Field averaging

By the broad concept of field averaging, we do not herein refer to any specific algorithm, but to the idea of studying permittivity as a relation between the electric displacement and the electric field averaged over a certain volume, that is,

$$\langle \mathbf{D} \rangle = \epsilon_{\text{eff}} \langle \mathbf{E} \rangle. \quad (5.14)$$

If an isotropic medium is considered, the effective permittivity is obtained from the ratio of scalar components as

$$\epsilon_{\text{eff}} = \frac{\langle D \rangle}{\langle E \rangle}. \quad (5.15)$$

Measuring the actual fields inside the material is practically nearly impossible. Therefore, the approaches to this kind of homogenization are usually analytical or computational. Several novel methods for metamaterial homogenization in a dynamic case have lately been proposed [20, 21, 91, 92, 111].

The field averaging method considered in Publication V in the Thesis is based on straightforward volume integration, such as

$$\epsilon_{\text{eff}} = \frac{\int D \, dV}{\int E \, dV}, \quad (5.16)$$

where the fields and their volume integrals are solved computationally. The integration volume is one unit cell, and the results from consecutive cells in the slab are averaged once more over all layers to obtain one effective permittivity value for the whole slab. It should be noted that this homogenization model is also based on resolving a local parameter ϵ_{eff} , which fails to represent any non-local effects.

The field averaging technique allows us to study each unit cell separately. In Publication V, we especially study the boundary effects of the composite slab. It is found that the layers on the boundary behave differently from the ones in the middle of the slab, which is in agreement with earlier theoretical results [112, 113]. It is also suggested that the homogenization models of composite media should include separate transition layers to characterize these boundary effects [19, 107]. Also, one approach is to define an effective thickness for the homogenized slab [106]. Nevertheless, a composite slab should include enough layers to make this boundary effect negligible and to behave as a bulk medium. This effect may be even more significant for metamaterials with resonant inclusions as shown in [114].

In Publication V, the comparison between the results of the NRW-technique and the field averaging is made. An obvious difference is that the field averaging yields smooth curves, which are not affected by the Fabry–Pérot resonances.

Moreover, the field averaging results suggest different effective parameters for the boundary layers. On the other hand, by field averaging, only the effective permittivity is obtained and with higher frequencies, the effective model does not replicate the scattering properties of the original composite very well.

The current challenge in homogenization theories and methods is the question how to correctly model the effects of weak spatial dispersion [19,21]. More precisely, the objective is to combine a physically sound effective material model with a reasonably simple retrieval algorithm.

6. Summary of the publications

Publication I: “Polarizability of a dielectric hemisphere”

This paper studies the electrostatic response of a dielectric hemispherical object. The response is considered by means of polarizability. Since a hemisphere is a three-dimensional object with rotational symmetry, its polarizability becomes a dyadic with two independent components, that is, the axial and the transverse polarizabilities. A semianalytical method for computing these polarizability components as a function of the relative electric permittivity is presented. The method is based on writing the potential function as analytical series expansions based on the eigensolutions of the Laplace equation in spherical coordinates. However, the coefficients of the expansions do not have closed-form expressions and they must be solved from a matrix equation which can be constructed by applying the electrostatic boundary conditions. The method provides high accuracy but, on the other hand, it requires using large matrices which consumes both time and memory. Also, both polarizability components must be solved separately from their own equations. Therefore, approximate formulas for the axial and the transverse polarizability are given. These easy-to-use formulas are based on Padé approximation and they are obtained by nonlinear data fitting.

Publication II: “Electrostatic resonances of a negative-permittivity hemisphere”

This paper expands the analysis of Publication I by considering a hemisphere with negative permittivity. Negative permittivity values are not physical in electrostatics, but for example for noble metals at optical and UV frequencies the real part of their complex permittivity may become negative. In this pa-

per it is assumed that the considered hemisphere is very small compared with the wavelength of the external electric field, so that the quasistatic analysis is still valid. It is found that the method presented in Publication I gives nonconvergent singular solutions between permittivity values $\epsilon_r = -3$ and $\epsilon_r = -1/3$. This is caused by the surface plasmons supported by the edge and the planar surface of the hemisphere. These resonant modes are also called electrostatic resonances. They are eigensolutions of Laplace equation on interfaces between media with permittivities of opposite signs which oscillate with arbitrary amplitude and spatial frequency without external excitation. Their occurrence depends on the geometry of the interface and the permittivity contrast.

It is shown that the sharp edge of the hemisphere supports even edge modes with $-3 < \epsilon_r < -1$ and odd edge modes with $-1 < \epsilon_r < -1/3$. At $\epsilon_r = -1$, surface modes occur on the planar surface of the hemisphere. The surface resonances are effectively attenuated by already small losses. However, the most efficient way to stabilize unphysically singular edge modes is to round the sharp edges when modeling objects with negative material parameters.

Publication III: “Electrostatic response of a half-disk”

This paper studies the electrostatic response of a half-disk which is a 2D version of a hemisphere considered in Publications I and II. A similar method for computing the polarizability components of a half-disk is derived. In this case, the solution is based on series expansions of eigensolutions of the Laplace equation in 2D polar coordinates. Again, the unknown coefficients are solved from a large matrix equation. The polarizability of a half-disk is determined by two orthogonal components which in this paper are named as series and parallel polarizabilities. Unlike in the case of a 3D hemisphere where the components had to be solved from separate equations, in 2D the orthogonal components are related and both of them can be obtained using the same equation. This follows from the so-called Keller–Dykhne–Mendelson duality relation of 2D geometries. Again, easy-to-use approximative formula for the polarizability is given.

Moreover, this paper studies the response of a negative-permittivity half-disk. The effects are very similar to the case of the 3D hemisphere. The sharp corners of the half-disk support even edge modes with $-3 < \epsilon_r < -1$ and odd edge modes with $-1 < \epsilon_r < -1/3$. However, near $\epsilon_r = -1$, the whole contour of the half-disk is capable of supporting resonant modes. Again, introducing losses and

rounding the corners is required to obtain converging and physically reasonable numerical results.

Publication IV: “Surface modes of negative-parameter interfaces and the importance of rounding sharp corners”

This paper gives a review of the surface plasmon resonances in cases of some of the most common canonical geometries. An electrostatic approach is used. On interfaces between materials with permittivities of opposite signs, solutions for Laplace equation may be found which can exist without external excitation, oscillate along the interface and decay away from it. In the dynamic case, these oscillations occur on a length scale notably smaller than the wavelength. Expressions for possible resonant modes are given for a half-space, a sphere, an ellipsoid, a circular cylinder and a sharp wedge. The resonant modes occurring on smooth surfaces are found to be very sensitive to losses. On the other hand, the response of a sharp negative-permittivity wedge is shown to be unphysically singular and also almost invulnerable to losses. Instead, an efficient way to stabilize to edge resonances is to round all sharp corners when modeling objects with negative permittivities.

Considering the importance of plasmonic resonances in numerical modeling, a couple of examples are computed using the finite element method (FEM). First, the effective permittivity of a 2D composite medium consisting of square cylinders with sharp corners and negative permittivity is studied. The 90° corners make the solution nonunique and nonconvergent for $-3 < \epsilon_r < -1/3$. It is seen how the rounding of the corners makes the solution convergent.

Furthermore, scattering of a plane wave from a negative-permittivity square cylinder is studied. Even though the surface resonances are very localized phenomena decaying exponentially away from the surface, it is observed that they cause unstabilities also to the far-field results. Again, the conclusion is that sharp corners must be rounded.

Publication V: “Homogenization of thin dielectric composite slabs: techniques and limitations”

This paper focuses on electromagnetic modeling of composite materials. The effective permittivity is retrieved for a thin slab consisting of a simple cubic lat-

tice of dielectric spheres in vacuum background. The effects of frequency and the slab thickness on the retrieval results are studied by two simple computational methods, namely the Nicolson–Ross–Weir (NRW) technique based on S-parameters and a straightforward field averaging technique. Simulations are performed using COMSOL MULTIPHYSICS, which is based on the finite element method (FEM). An analytical mixing formula estimate is used as a (quasi)static reference value for the corresponding bulk material.

The NRW technique gives both permittivity ϵ_{eff} and permeability μ_{eff} . In this lossless case, the results are found suffering from Fabry–Pérot resonances which occur when the total thickness of the slab equals an integer multiple of a half wavelength ($\lambda/2$). Moreover, the retrieved material parameters show unphysical anti-resonant dispersion, which violates the principle of causality.

The applied averaging method is based on the field integration over the unit cells. By this technique the cells of the slab can be studied separately. It is found that the unit cells on the boundary of the slab have stronger response than the ones inside the slab. Therefore, a thin slab has higher permittivity compared with bulk material as the boundary layers increase the average permittivity of the slab. The simulations confirm that the permittivity of the slab in the (quasi)static limit depends on the number of consecutive layers in the slab. That is, enough layers are needed for the slab to behave as a bulk medium.

The main conclusion is that in order to consider a composite material homogeneous, the unit cells must remain very small compared with the wavelength. If the electrical size of the unit cells exceeds $\lambda/20$, the homogeneity assumption may no further be valid. On the other hand, when decreasing the unit cell size, the quasistatic limit where analytical electrostatic mixing rules are applicable is reached not until $\lambda/100$. The NRW technique can safely be used sufficiently below the first Fabry–Pérot resonance. However, the studied slab must include enough layers, preferably 10 or more, to resemble bulk material but at the same time the total thickness of the slab must remain below $\lambda/2$. Both these restrictions limit the size of a single unit cell.

Publication VI: “Quasi-dynamic homogenization of geometrically simple dielectric composites”

Similarly to Publication V, this article studies the homogenization of a dielectric slab consisting of a simple cubic lattice of dielectric spheres. For the finite-thickness slab, the Nicolson–Ross–Weir retrieval technique based on S-

parameters is applied. The objective of this paper is to study alternative ways to retrieve the effective permittivity ϵ_{eff} to eliminate the distortion caused by the half-wavelength Fabry–Pérot resonances. Also, the frequency dispersion of the effective permittivity of the slab is studied. A frequency limit for a 1% deviation from the static Lord Rayleigh estimate is sought. Furthermore, the permittivity of an infinite lattice is studied by eigenfrequency analysis for a single unit cell. The simulations are performed using the frequency-domain solver of CST MICROWAVE STUDIO.

By assuming the slab non-magnetic, $\mu_{\text{eff}} = 1$, the permittivity can be retrieved from either only reflection (S_{11}) or transmission (S_{21}) data. The smoothest and most physical-looking curve can however be obtained as a square of the refractive index n that is computed using both S-parameters. Also, the otherwise unwanted Fabry–Pérot resonances allow us to retrieve the effective permittivity at discrete points exactly at the resonance.

The eigenfrequency analysis of the unit cell indicates that the effect of spatial dispersion in the composite is much weaker than the deviation from the static limit value due to the frequency dispersion. However, a simple universal rule for the 1% tolerance limit for analytical static mixing formulas cannot be formed since the dispersion seems to strongly depend on the volume fraction and the permittivity of the inclusions.

Bibliography

- [1] A. Sihvola, "Dielectric polarization and particle shape effects," *J. Nanomaterials*, vol. 2007, no. 2, pp. 45090:1–9, 2007.
- [2] G. V. Eleftheriades and K. G. Balmain, eds., *Negative-Refractive Metamaterials: Fundamental Principles and Applications*. Hoboken, NJ: Wiley, 2005.
- [3] N. Engheta and R. W. Ziolkowski, eds., *Metamaterials: Physics and Engineering Explorations*. Hoboken, NJ: Wiley-Interscience, 2006.
- [4] C. Caloz and T. Itoh, *Electromagnetic Metamaterials: Transmission Line Theory and Microwave Applications*. Hoboken, NJ: Wiley-Interscience, 2006.
- [5] A. K. Sarychev and V. M. Shalaev, *Electrodynamics of Metamaterials*. Singapore: World Scientific, 2007.
- [6] R. Marqués, F. Martín, and M. Sorolla, eds., *Metamaterials with Negative Parameters*. Hoboken, NJ: Wiley-Interscience, 2008.
- [7] M. Lapine and S. Tretyakov, "Contemporary notes on metamaterials," *IET Microw. Antennas Propag.*, vol. 1, pp. 3–11, Feb. 2007.
- [8] J. M. Pitarke, V. M. Silkin, E. V. Chulkov, and P. M. Echenique, "Theory of surface plasmons and surface-plasmon polaritons," *Rep. Prog. Phys.*, vol. 70, pp. 1–87, Jan. 2007.
- [9] S. A. Maier, *Plasmonics: Fundamentals and Applications*. New York: Springer, 2007.
- [10] D. R. Fredkin and I. D. Mayergoyz, "Resonant behavior of dielectric objects (electrostatic resonances)," *Phys. Rev. Lett.*, vol. 91, pp. 253902:1–4, Dec. 2003.
- [11] G. W. Milton, *The Theory of Composites*. Cambridge: Cambridge Univ. Press, 2002.
- [12] A. Sihvola, *Electromagnetic Mixing Formulas and Applications*. London: IEE, 1999.
- [13] A. M. Nicolson and G. F. Ross, "Measurement of the intrinsic properties of materials by time-domain techniques," *IEEE Trans. Inst. Meas.*, vol. IM-19, pp. 377–382, Nov. 1970.
- [14] W. B. Weir, "Automatic measurement of complex dielectric constant and permeability at microwave frequencies," *Proc. IEEE*, vol. 62, pp. 33–36, Jan. 1974.

- [15] J. D. Jackson, *Classical Electrodynamics*. New York: Wiley, 3rd ed., 1999.
- [16] I. V. Lindell, *Methods for Electromagnetic Field Analysis*. New York: IEE, 2nd ed., 1995.
- [17] A. Serdyukov, I. Semchenko, S. Tretyakov, and A. Sihvola, *Electromagnetics of Bi-Anisotropic Materials*. Amsterdam: Gordon and Breach Science Publ., 2001.
- [18] I. V. Lindell, A. H. Sihvola, S. A. Tretyakov, and A. J. Viitanen, *Electromagnetic Waves in Chiral and Bi-Isotropic Media*. Boston: Artech House, 1994.
- [19] C. R. Simovski, "On electromagnetic characterization and homogenization of nanostructured metamaterials," *J. Opt.*, vol. 13, pp. 013001:1–22, Jan. 2011.
- [20] C. Fietz and G. Shvets, "Current-driven metamaterial homogenization," *Physica B*, vol. 405, pp. 2930–2934, July 2010.
- [21] A. Alù, "Restoring the physical meaning of metamaterial constitutive parameters," *Phys. Rev. B*, vol. 83, pp. 081102(R):1–4, Feb. 2011.
- [22] J. Vanderlinde, *Classical electromagnetic theory*. Singapore: Wiley, 1993.
- [23] A. Sihvola, "Ubi materia, ibi geometria." Helsinki University of Technology, Electromagnetics Laboratory Report Series, No. 339, Sept. 2000. Revised and expanded version online: <http://users.tkk.fi/asihvola/umig.pdf>.
- [24] J. Venermo and A. Sihvola, "Dielectric polarizability of circular cylinder," *J. Electrostat.*, vol. 63, pp. 101–117, Feb. 2005.
- [25] M. L. Mansfield, J. F. Douglas, and E. J. Garboczi, "Intrinsic viscosity and the electrical polarizability of arbitrarily shaped objects," *Phys. Rev. E*, vol. 64, pp. 061401:1–16, Nov. 2001.
- [26] A. Sihvola, P. Ylä-Oijala, S. Järvenpää, and J. Avelin, "Polarizabilities of platonic solids," *IEEE Trans. Antennas. Propag.*, vol. 52, pp. 2226–2233, Sept. 2004.
- [27] B. U. Felderhof and D. Palaniappan, "Longitudinal and transverse polarizability of the conducting double sphere," *J. Appl. Phys.*, vol. 88, pp. 4947–4952, Nov. 2000.
- [28] H. Wallén and A. Sihvola, "Polarizability of conducting sphere-doublets using series of images," *J. Appl. Phys.*, vol. 96, pp. 2330–2335, Aug. 2004.
- [29] M. Pitkonen, "An explicit solution for the electric potential of the asymmetric dielectric double sphere," *J. Phys. D: Appl. Phys.*, vol. 40, pp. 1483–1488, Feb. 2007.
- [30] M. Pitkonen, "Polarizability of a pair of touching dielectric spheres," *J. Appl. Phys.*, vol. 103, pp. 104910:1–7, May 2008.
- [31] M. Schiffer and G. Szegő, "Virtual mass and polarization," *Trans. Am. Math. Soc.*, vol. 67, pp. 130–205, Sept. 1949.
- [32] J. Avelin, *Polarizability Analysis of Canonical Dielectric and Bi-Anisotropic Scatterers*. PhD thesis, Helsinki University of Technology, Electromagnetics Laboratory Report Series, Report 414, Sept. 2003. Available online: <http://lib.tkk.fi/Diss/2003/isbn9512268361/>.

- [33] M. Pitkonen, *Exact Solutions for Some Spherical Electrostatic Scattering Problems*. PhD thesis, Aalto University School of Science and Technology, TKK Radio Science and Engineering Publications, Report R14, May 2010. Available online: <http://lib.tkk.fi/Diss/2010/isbn9789526030579/>.
- [34] M. Pitkonen, "A closed-form solution for the polarizability of a dielectric double half-cylinder," *J. Electromagn. Waves and Appl.*, vol. 24, pp. 1267–1277, May 2010.
- [35] J. Aizpurua, A. Rivacoba, and P. Apell, "Electron-energy losses in hemispherical targets," *Phys. Rev. B*, vol. 54, pp. 2901–2909, July 1996.
- [36] D. S. Jones, "Low frequency electromagnetic radiation," *IMA J. Appl. Math.*, vol. 23, no. 4, pp. 421–447, 1979.
- [37] A. Mejdoubi and C. Brosseau, "Finite-element simulation of the depolarization factor of arbitrarily shaped inclusions," *Phys. Rev. E*, vol. 74, pp. 031405:1–13, Sept. 2006.
- [38] A. Sihvola and J. Venermo, "Boosting numerical accuracy in calculation of polarizability of two-dimensional scatterers," *IEEE Antennas Propag. Mag.*, vol. 47, pp. 60–65, Oct. 2005.
- [39] J. B. Keller, "Conductivity of a medium containing a dense array of perfectly conducting spheres or cylinders or nonconducting cylinders," *J. Appl. Phys.*, vol. 34, pp. 991–993, Apr. 1963.
- [40] A. M. Dykhne, "Conductivity of a two-dimensional two-phase system," *Sov. Phys. JETP*, vol. 32, no. 1, pp. 63–65, 1970. [Originally published in *Zh. Eksp. Teor. Fiz.*, vol. 59, pp. 110–115, 1970 (In Russian)].
- [41] K. S. Mendelson, "A theorem on the effective conductivity of a two-dimensional heterogeneous medium," *J. Appl. Phys.*, vol. 46, pp. 4740–4741, Nov. 1975.
- [42] V. G. Veselago, "The electrodynamics of substances with simultaneously negative values of ϵ and μ ," *Sov. Phys. Uspekhi*, vol. 10, no. 4, pp. 509–514, 1968. [Originally published in *Usp. Fiz. Nauk.*, vol. 92, pp. 517–526, 1967 (In Russian)].
- [43] S. Tretyakov, *Analytical Modeling in Applied Electromagnetics*. Norwood, MA: Artech House, 2003.
- [44] C. F. Bohren and D. R. Huffman, *Absorption and Scattering of Light by Small Particles*. New York: Wiley, 1998.
- [45] P. B. Johnson and R. W. Christy, "Optical constants of the noble metals," *Phys. Rev. B*, vol. 6, pp. 4370–4379, Dec. 1972.
- [46] H. A. Atwater, "The promise of plasmonics," *Sci. Am.*, vol. 296, pp. 56–63, Apr. 2007.
- [47] M. Pelton, J. Aizpurua, and G. Bryant, "Metal-nanoparticle plasmonics," *Laser & Photon. Rev.*, vol. 2, pp. 136–159, Apr. 2008.
- [48] I. Freestone, N. Meeks, M. Sax, and C. Higgitt, "The Lycurgus cup - a roman nanotechnology," *Gold Bulletin*, vol. 40, no. 4, pp. 270–277, 2007.
- [49] J. B. Pendry, "Negative refraction makes a perfect lens," *Phys. Rev. Lett.*, vol. 85, pp. 3966–3969, Oct. 2000.

- [50] D. R. Smith, W. J. Padilla, D. C. Vier, S. C. Nemat-Nasser, and S. Schultz, "Composite medium with simultaneously negative permeability and permittivity," *Phys. Rev. Lett.*, vol. 84, pp. 4184–4187, May 2000.
- [51] J. B. Pendry, A. J. Holden, D. J. Robbins, and W. J. Stewart, "Magnetism for conductors and enhanced nonlinear phenomena," *IEEE Trans. Microwave Theory Tech.*, vol. 47, pp. 2075–2084, Nov. 1999.
- [52] R. A. Shelby, D. R. Smith, and S. Schultz, "Experimental verification of a negative index of refraction," *Science*, vol. 292, pp. 77–79, Apr. 2001.
- [53] A. Sihvola and S. Zouhdi, "Handedness in plasmonics: electrical engineers' perspective," in *Metamaterials and Plasmonics: Fundamentals, Modelling, Applications* (S. Zouhdi, A. Sihvola, and A. P. Vinogradov, eds.), NATO SPS Ser. B, pp. 3–20, Dordrecht: Springer, 2009.
- [54] J. B. Pendry, D. Schurig, and D. R. Smith, "Controlling electromagnetic fields," *Science*, vol. 312, pp. 1780–1782, May 2006.
- [55] U. Leonhardt, "Optical conformal mapping," *Science*, vol. 312, pp. 1777–1780, May 2006.
- [56] D. Schurig, J. J. Mock, B. J. Justice, S. A. Cummer, J. B. Pendry, A. F. Starr, and D. R. Smith, "Metamaterial electromagnetic cloak at microwave frequencies," *Science*, vol. 314, pp. 977–980, Nov. 2006.
- [57] A. Alù and N. Engheta, "Achieving transparency with plasmonic and metamaterial coatings," *Phys. Rev. E*, vol. 72, pp. 016623:1–9, July 2005.
- [58] A. Alù and N. Engheta, "Plasmonic cloaks," in *Metamaterials and Plasmonics: Fundamentals, Modelling, Applications* (S. Zouhdi, A. Sihvola, and A. P. Vinogradov, eds.), NATO SPS Ser. B, pp. 37–47, Dordrecht: Springer, 2009.
- [59] P. Alitalo, *Microwave Transmission-Line Networks for Backward-Wave Media and Reduction of Scattering*. PhD thesis, Helsinki University of Technology, TKK Radio Science and Engineering Publications, Report R8, July 2009. Available online: <http://lib.tkk.fi/Diss/2009/isbn9789512299874/>.
- [60] S. Zhang, W. Fan, K. J. Malloy, S. R. J. Brueck, N. C. Panoiu, and R. M. Osgood, "Near-infrared double negative metamaterials," *Opt. Express*, vol. 13, pp. 4922–4930, June 2005.
- [61] G. Dolling, M. Wegener, C. M. Soukoulis, and S. Linden, "Negative-index metamaterial at 780 nm wavelength," *Opt. Lett.*, vol. 32, pp. 53–55, Jan. 2007.
- [62] J. Valentine, S. Zhang, T. Zentgraf, E. Ulin-Avila, D. A. Genov, G. Bartal, and X. Zhang, "Three-dimensional optical metamaterial with a negative refractive index," *Nature*, vol. 455, pp. 376–379, Sept. 2008.
- [63] B. A. Munk, *Metamaterials: Critique and Alternatives*. Hoboken, NJ: Wiley, 2009.
- [64] M. Gustafsson and D. Sjöberg, "Sum rules and physical bounds on passive metamaterials," *New J. Phys.*, vol. 12, pp. 043046:1–18, Apr. 2010.
- [65] J. Skaar and K. Seip, "Bounds for the refractive indices of metamaterials," *J. Phys. D: Appl. Phys.*, vol. 39, pp. 1226–1229, Mar. 2006.

- [66] Ø. Lind-Johansen, K. Seip, and J. Skaar, "The perfect lens on a finite bandwidth," *J. Math. Phys.*, vol. 50, pp. 012908:1–9, Jan. 2009.
- [67] J. T. Shen and P. M. Platzman, "Near field imaging with negative dielectric constant lenses," *Appl. Phys. Lett.*, vol. 80, pp. 3286–3288, May 2002.
- [68] D. R. Smith, D. Schurig, M. Rosenbluth, S. Schultz, S. A. Ramakrishna, and J. B. Pendry, "Limitations on subdiffraction imaging with a negative refractive index slab," *Appl. Phys. Lett.*, vol. 82, pp. 1506–1508, Mar. 2003.
- [69] V. A. Podolskiy and E. E. Narimanov, "Near-sighted superlens," *Opt. Lett.*, vol. 30, pp. 75–77, Jan. 2005.
- [70] C. Menzel, T. Paul, C. Rockstuhl, T. Pertsch, S. Tretyakov, and F. Lederer, "Validity of effective material parameters for optical fishnet metamaterials," *Phys. Rev. B*, vol. 81, pp. 035320:1–5, Jan. 2009.
- [71] R. H. Ritchie, "Plasma losses by fast electrons in thin films," *Phys. Rev.*, vol. 106, pp. 874–881, June 1957.
- [72] E. A. Stern and R. A. Ferrell, "Surface plasma oscillations of a degenerate electron gas," *Phys. Rev.*, vol. 120, pp. 130–136, Oct. 1960.
- [73] J. Homola, ed., *Surface Plasmon Resonance Based Sensors*. Berlin: Springer, 2006.
- [74] E. Özbay, "Plasmonics: merging photonics and electronics at nanoscale dimensions," *Science*, vol. 311, pp. 189–193, Jan. 2006.
- [75] P. K. Jain, X. Huang, I. H. El-Sayed, and M. A. El-Sayed, "Review of some interesting surface plasmon resonance-enhanced properties of noble metal nanoparticles and their applications to biosystems," *Plasmonics*, vol. 2, pp. 107–118, July 2007.
- [76] L. R. Hirsch, R. J. Stafford, J. A. Bankson, S. R. Sershen, B. Rivera, R. E. Price, J. D. Hazle, N. J. Halas, and J. L. West, "Nanoshell-mediated near-infrared thermal therapy of tumors under magnetic resonance guidance," *Proc. Natl. Acad. Sci. USA*, vol. 100, pp. 13549–13554, Nov. 2003.
- [77] C. Loo, A. Lowery, N. Halas, J. West, and R. Drezek, "Immunotargeted nanoshells for integrated cancer imaging and therapy," *Nano Lett.*, vol. 5, pp. 709–711, Mar. 2005.
- [78] K. Okamoto, I. Niki, A. Shvartser, Y. Narukawa, T. Mukai, and A. Scherer, "Surface-plasmon-enhanced light emitters based on InGaN quantum wells," *Nature Mater.*, vol. 3, pp. 601–605, Sept. 2004.
- [79] H. A. Atwater and A. Polman, "Plasmonics for improved photovoltaic devices," *Nature Mater.*, vol. 9, pp. 205–213, Mar. 2010.
- [80] B. E. Sernelius, *Surface Modes in Physics*. Berlin: Wiley-VCH, 2001.
- [81] A. Moussiaux, A. Ronveaux, and A. Lucas, "Surface plasmon oscillations for different geometrical shapes," *Can. J. Phys.*, vol. 55, no. 16, pp. 1423–1433, 1977.
- [82] L. Dobrzynski and A. A. Maradudin, "Electrostatic edge modes in a dielectric wedge," *Phys. Rev. B*, vol. 6, pp. 3810–3815, Nov. 1972.

- [83] J. H. Hetherington and M. F. Thorpe, "The conductivity of a sheet containing inclusions with sharp corners," *Proc. R. Soc. A*, vol. 438, pp. 591–604, Sept. 1992.
- [84] L. C. Davis, "Electrostatic edge modes of a dielectric wedge," *Phys. Rev. B*, vol. 14, pp. 5523–5525, Dec. 1976.
- [85] A. A. Sukhorukov, I. V. Shadrivov, and Y. S. Kivshar, "Wave scattering by meta-material wedges and interfaces," *Int. J. Numer. Model.*, vol. 19, pp. 105–117, mar–apr 2006.
- [86] J. Helsing and R. Ojala, "Corner singularities for elliptic problems: Integral equations, graded meshes, quadrature, and compressed inverse preconditioning," *J. Comput. Phys.*, vol. 227, pp. 8820–8840, Oct. 2008.
- [87] J. Helsing, "The effective conductivity of arrays of squares: Large random unit cells and extreme contrast ratios," *J. Comput. Phys.*, vol. 230, pp. 7533–7547, Aug. 2011.
- [88] J. Helsing, R. C. McPhedran, and G. W. Milton, "Spectral super-resolution in metamaterial composites." Submitted to *New J. Phys.*, arXiv:1105.5012v1, 2011.
- [89] C. Brosseau, "Modelling and simulation of dielectric heterostructures: a physical survey from an historical perspective," *J. Phys. D: Appl. Phys.*, vol. 39, pp. 1277–1294, Mar. 2006.
- [90] L. Jylhä, *Modeling of Electrical Properties of Composites*. PhD thesis, Helsinki University of Technology, TKK Radio Science and Engineering Publications, Report R1, Mar. 2008. Available online: <http://lib.tkk.fi/Diss/2008/isbn9789512292387/>.
- [91] M. G. Silveirinha, "Metamaterial homogenization approach with application to the characterization of microstructured composites with negative parameters," *Phys. Rev. B*, vol. 75, pp. 115104:1–15, Mar. 2007.
- [92] M. G. Silveirinha, "Generalized Lorentz–Lorenz formulas for microstructured materials," *Phys. Rev. B*, vol. 76, pp. 245117:1–9, Dec. 2007.
- [93] D. Sjöberg, "Determination of propagations constants and material data from waveguide measurements," *Progress in Electromagnetics Research B*, vol. 12, pp. 163–182, 2009.
- [94] D. Sjöberg and C. Larsson, "Characterization of composite materials in waveguides," in *2010 URSI International Symposium on Electromagnetics Theory (EMTS)*, pp. 592–595, 2010.
- [95] J. Baker-Jarvis, E. J. Vanzura, and W. A. Kissick, "Improved technique for determining complex permittivity with the transmission/reflection method," *IEEE Trans. Microwave Theory Tech.*, vol. 38, pp. 1096–1103, Aug. 1990.
- [96] R. E. Collin, *Foundations for Microwave Engineering*. Hoboken, NJ: Wiley–Interscience, 2nd ed., 2001.
- [97] J. C. Maxwell Garnett, "Colours in metal glasses and metal films," *Trans. R. Soc.*, vol. CCIII, pp. 385–420, 1904.
- [98] Lord Rayleigh, "On the influence of obstacles arranged in rectangular order upon the properties of the medium," *Phil. Mag.*, vol. 34, pp. 481–502, 1892.

- [99] R. C. McPhedran and D. R. McKenzie, “The conductivity of lattices of spheres I. The simple cubic lattice,” *Proc. R. Soc. Lond. A*, vol. 359, pp. 45–63, 1978.
- [100] D. A. G. Bruggeman, “Berechnung verschiedener physikalischer Konstanten von heterogenen Substanzen. I. Dielektrizitätskonstanten und Leitfähigkeiten der Mischkörper aus isotropen Substanzen,” *Ann. Phys. (Berlin)*, vol. 416, no. 7–8, pp. 636–679, 1935. [Originally: *Annalen der Physik*, 5. Folge, Band 24, Heft 7, pp. 636–664 and Heft 8, pp. 665–679, (1935)].
- [101] G. Grimvall, *Thermophysical Properties of Materials*. Amsterdam: North-Holland, 1986.
- [102] R. C. McPhedran and D. R. McKenzie, “Electrostatic and optical resonances of arrays of cylinders,” *Appl. Phys.*, vol. 23, pp. 223–235, 1980.
- [103] R. Ruppin, “Evaluation of extended Maxwell–Garnett theories,” *Opt. Comm.*, vol. 182, pp. 273–279, Aug. 2000.
- [104] H. Wallén, H. Kettunen, and A. Sihvola, “Mixing formulas and plasmonic composites,” in *Metamaterials and Plasmonics: Fundamentals, Modelling, Applications* (S. Zouhdi, A. Sihvola, and A. P. Vinogradov, eds.), NATO SPS Ser. B, pp. 91–102, Dordrecht: Springer, 2009.
- [105] D. R. Smith, S. Schultz, P. Markoš, and C. M. Soukoulis, “Determination of effective permittivity and permeability of metamaterials from reflection and transmission coefficients,” *Phys. Rev. B*, vol. 65, pp. 195104:1–5, Apr. 2002.
- [106] X. Chen, T. M. Grzegorzcyk, B.-I. Wu, J. Pacheco, Jr., and J. A. Kong, “Robust method to retrieve the constitutive effective parameters of metamaterials,” *Phys. Rev. E*, vol. 70, pp. 016608:1–7, July 2004.
- [107] C. R. Simovski, “Material parameters of metamaterials (a review),” *Opt. Spectrosc.*, vol. 107, pp. 726–753, Nov. 2009. [Originally published in *Optika i Spektroskopiya*, vol. 107, no. 5, pp. 766–793, 2009, (In Russian)].
- [108] Z. Szabó, G.-H. Park, R. Hedge, and E.-P. Li, “A unique extraction of metamaterial parameters based on Kramers–Kronig relationship,” *IEEE Trans. Microwave Theory Tech.*, vol. 58, pp. 2646–2653, Oct. 2010.
- [109] A.-H. Boughriet, C. Legrand, and A. Chapoton, “Noniterative stable transmission/reflection method for low-loss material complex permittivity determination,” *IEEE Trans. Microwave Theory Tech.*, vol. 45, pp. 52–57, Jan. 1997.
- [110] T. Koschny, P. Markoš, D. R. Smith, and C. M. Soukoulis, “Resonant and antiresonant frequency dependence of the effective parameters of metamaterials,” *Phys. Rev. E*, vol. 68, pp. 065602(R):1–4, Dec. 2003. [See also R. A. Depine and A. Lakhtakia, *Phys. Rev. E*, vol. 70, 048601, 2007; A. L. Efros, *Phys. Rev. E*, vol. 70, 048602, 2007; T. Koschny, P. Markoš, D. R. Smith and C. M. Soukoulis, *Phys. Rev. E*, vol. 70, 048603, 2007].
- [111] D. R. Smith and J. B. Pendry, “Homogenization of metamaterials by field averaging,” *J. Opt. Soc. Am. B*, vol. 23, pp. 391–403, Mar. 2006.
- [112] G. D. Mahan and G. Obermair, “Polaritons at surfaces,” *Phys. Rev.*, vol. 183, pp. 834–841, July 1969.

- [113] C. R. Simovski, S. A. Tretyakov, A. H. Sihvola, and M. M. Popov, "On the surface effect in thin molecular or composite layer," *Eur. Phys. J. AP*, vol. 9, pp. 195–204, Mar. 2000.
- [114] C. Rockstuhl, T. Paul, F. Lederer, T. Pertsch, T. Zentgraf, T. P. Meyrath, and H. Giessen, "Transition from thin-film to bulk properties of metamaterials," *Phys. Rev. B*, vol. 77, pp. 035126:1–9, Jan. 2008.

Errata

Publication I

Publication I already includes a published erratum [*J. Appl. Phys.*, vol. 102, no. 11, 119902, 2007]. However, two additional corrections are required. In the Appendix, on page 6, the factor $(-1)^m$ should be omitted from equation (A3). The corrected version of the formula which is used for computing the associated Legendre functions in this paper should read

$$P_n^m(\xi) = (1 - \xi^2)^{m/2} \frac{d^m}{d\xi^m} P_n(\xi).$$

Also, on page 4, the term 2^0 should be excluded from the list $N = 2^0, 2^1, 2^2, \dots, 2^{12}$.

Publication V

In the original published version of the article, several letters, mostly related to ligatures, are missing in the text. This is apparently due to a font problem. For the readers' convenience, the missing letters are filled in in the version included in the Thesis.

Also, on page 183, below Figure 9, it should read 'electric displacement **D**', not 'displacement current **D**'.

Publication VI

The paper and page numbers are confusingly combined in references [2,5,7–9,14,15]. The corrected page numbers should read: [2] pp. 0138071:1–11, [5] pp. 041101:1–4, [7] pp. 036617:1–11, [8] pp. 035320:1–5, [9] RS6S21:1–40, [14] pp. 195104:1–5, and [15] pp. 016608:1–7

How to solve the polarizability of a hemisphere? What are surface plasmons, or electrostatic resonances? Can a composite slab be modeled as an effectively homogeneous medium? How are its effective material parameters then retrieved, and what are the limitations of this homogenization procedure? We find out that even simple geometries can sometimes behave in a complex way.



ISBN 978-952-60-4337-1 (pdf)

ISBN 978-952-60-4336-4

ISSN-L 1799-4934

ISSN 1799-4942 (pdf)

ISSN 1799-4934

Aalto University
School of Electrical Engineering
Department of Radio Science and Engineering
www.aalto.fi

**BUSINESS +
ECONOMY**

**ART +
DESIGN +
ARCHITECTURE**

**SCIENCE +
TECHNOLOGY**

CROSSOVER

**DOCTORAL
DISSERTATIONS**